I&EC research
Industrial & Engineering Chemistry Research

pubs.acs.org/IECR
Article

Process Modeling and Techno-economic Analysis of an Integrated Large-Scale CO_2/CO Electroreduction Plant to Produce C_{2+} Products

Asvin Sajeev, Matthijs Kroes, Isabell Bagemihl, Ruud Kortlever, Wiebren de Jong, and Mahinder Ramdin*

Cite This: *Ind. Eng. Chem. Res.* 2026, 65, 1716−1733
Read Online

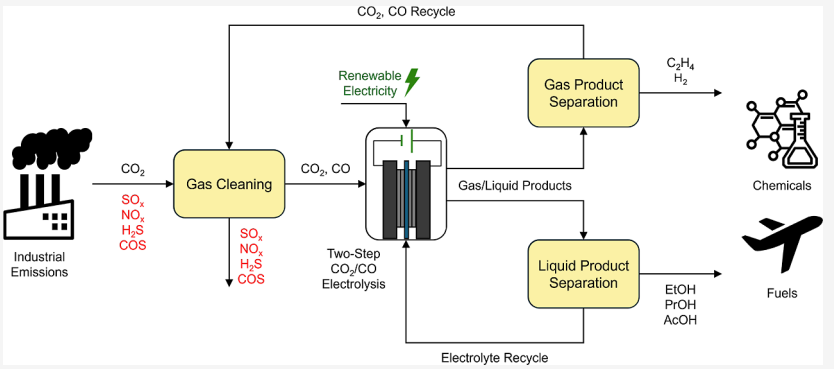

ABSTRACT: CO_2 feedstock obtained from point sources, such as chemical industries or fossil fuel-based power plants, typically contains gaseous contaminants such as SO_x, NO_x, H_2S, and COS, which can be detrimental to the catalysts used to electrochemically convert CO_2/CO into valuable fuels and chemicals. A significant suppression of C_{2+} products is observed even in the presence of 10 ppm of these impurities due to catalyst poisoning and a selectivity change. Hence, it is necessary to have an upstream cleaning process to maintain a high selectivity toward high value C_{2+} products and to reduce the operational costs associated with frequent catalyst regeneration or replacement. We present a comprehensive process model and technoeconomic analysis of an integrated large-scale two-step CO_2/CO electroreduction plant that produces C_{2+} products including ethylene, acetic acid, ethanol, and *n*-propanol, using blast furnace gas obtained from a steel manufacturing facility as feedstock. Detailed modeling and integration of the upstream cleaning units, CO_2/CO electrolyzers, and the downstream separation of gas/liquid products are performed using Aspen Plus. Our analysis shows that the large-scale two-step CO_2/CO electroreduction process is not profitable under the base case scenario and requires significant improvements in electrolyzer performance, reduction in capital costs, and favorable market conditions to improve the economics. The upstream cleaning units only contribute to ∼15% of the CAPEX and ∼8% OPEX of the entire plant, while the electrolyzers contribute to ∼63% of the total CAPEX and OPEX. A positive net present value ($54M), a payback time of 13 years, and an internal rate of return of 12.8% can be achieved when the electrolyzer capital cost is $10,000/m^2 (−50%) and electricity price is $20/MWh (−50%), with current densities of 750 mA/cm^2 (+50%) for both electrolyzers and cell voltages of 2.5 V (−17%) for CO_2R and 2.0 V (−20%) for COR electrolyzers, and when the product prices are 35% higher than the current market prices. Incorporating an energy-saving coelectrolysis process or integration into facilities that can directly utilize the products can accelerate the commercialization of the two-step CO_2/CO electroreduction process.

1. INTRODUCTION

The increasing concentration of CO_2 in the atmosphere, largely driven by industrial emissions, is a major driver of climate change, necessitating urgent and innovative strategies for its reduction.[1] Among various CO_2 conversion technologies, the electrochemical reduction of CO_2 to C_{2+} products presents a promising pathway for mitigating CO_2 emissions and simultaneously producing valuable chemicals and fuels, utilizing electricity generated from renewable energy sources such as wind and solar.[2,3] Some of the key advantages of electrochemical CO_2 reduction (CO_2R) include (i) the ability to control the reaction rates and selectivities through the external applied voltage, (ii) modularity and scalability of electrolyzer stacks, and (iii) the production of a range of C_1−C_3 gaseous and liquid products.[4−7] Despite these promising prospects, scaling-up of

Received: July 23, 2025
Revised: November 3, 2025
Accepted: December 9, 2025
Published: January 14, 2026

this technology for industrial applications would require optimization on the molecular level (mechanism, catalyst, and electrolyte), the electrolyzer level (cell design and configuration) and the process level (upstream and downstream processes), to increase the selectivity, energy efficiency, and operational stability while reducing the capital and operating costs.[8]

Recent research has primarily focused on optimizing the design of lab-scale electrolyzer flow systems, electrocatalyst materials, and understanding the complex reaction mechanisms, in an effort to improve the current density and selectivity of CO_2R.[9−13] However, there is limited research on the process modeling and techno-economic optimization of the overall process, especially integrating the upstream gas cleaning units. CO_2 feedstocks obtained from point sources such as chemical industries or fossil fuel-based power plants typically contain gaseous contaminants such as SO_x, NO_x, H_2S, and COS.[14,15] Studies have shown the detrimental effect of these gaseous contaminants on CO_2R using copper catalysts, where a significant suppression of C_{2+} products is observed due to catalyst poisoning and selectivity change, even in the presence of 10 ppm of these impurities.[16−20] Thus, developing catalysts resistant to poisoning or removing these contaminants from industry-supplied CO_2 feedstocks will be necessary to maintain a high selectivity toward C_{2+} products as well as to reduce the operational costs associated with frequent catalyst regeneration or replacement.[20]

Several studies have reported the techno-economics of CO_2R to specific products such as ethylene or formic acid; however, none of these consider the integration of electrolyzers with realistic upstream and downstream processing units, which is crucial for developing a robust and scalable CO_2R plant that can operate efficiently under industrial conditions.[21−29] Here, we present a comprehensive process model and techno-economic analysis of an integrated large-scale two-step CO_2/CO electroreduction plant that produces C_{2+} products including ethylene, acetic acid, ethanol, and *n*-propanol. The process model includes detailed modeling and analysis of the upstream gas cleaning units, CO_2 capture, electrochemical reduction of CO_2/CO, recycling of unreacted CO_2/CO, and downstream gas/liquid product separation, using the process simulation software Aspen Plus. The selection of technologies for upstream cleaning, CO_2/CO electrolyzers, and downstream units is based on the currently best available technology at the industrial scale or established/scalable lab-scale technologies. The entire CO_2R plant is considered to be integrated with an existing manufacturing facility such as a steel plant, where the byproduct gas generated in the facility will be used as feedstock for CO_2R. By modeling the entire process chain, we aim to provide insights into the operational parameters and economic feasibility, identify potential bottlenecks, and guide future research and development efforts in the commercialization of the CO_2R process.

2. BACKGROUND AND STATE OF THE ART

The electrochemical reduction of CO_2 can be performed on a range of electrocatalytic materials including metals such as Sn, Ag, Au, and Cu, nonmetallic materials such as nitrogen-doped carbon and metal−organic frameworks, and molecular catalysts.[30−32] However, Cu and Cu-based materials are the only group of catalysts known to reduce CO_2 or CO to C_{2+} products with a reasonably high selectivity.[33,34] Typical current densities achieved during CO_2R with traditional H-cell type electrolyzers are below 30 mA/cm^2, while industrial-scale water electrolyzers achieve more than 1000 mA/cm^2.[33,35] Several studies have reported current densities above 200 mA/cm^2 for CO_2R to C_{2+} products using copper-based catalysts and gas diffusion electrode (GDE) or membrane electrode assembly (MEA)-based cells, as shown in Table S1.[36−43] Studies have also reported current densities above 200 mA/cm^2 for electrochemical CO reduction (COR) to C_{2+} products using similar catalysts and cell configurations (see Table S2) but with higher faradaic efficiencies (FE) toward C_{2+} products, lower cell potentials, higher single pass conversions, and higher reactant utilization compared to CO_2R.[44−49] This is mainly attributed to the lower number of electrons required for COR products, higher reactivity of CO, and the absence of parasitic reactions with the electrolyte.

Furthermore, the performance of a CO_2R/COR electrolyzer is highly dependent on the quality of the feedstock as the presence of various contaminants impacts the system in different ways. Inert gases, such as N_2, dilute the feedstock and reduce the partial pressure of CO_2/CO, resulting in lower CO_2/CO reduction rates and increased hydrogen evolution reaction (HER).[50,51] Reducible gases, such as NO_x, compete and consume electrons under CO_2R/COR conditions, reducing the overall FE toward desired products.[16,18] Some reducible gases, such as SO_x, also bind strongly with the catalyst to block the active sites or modify the catalyst properties, altering the selectivity of CO_2R/COR. Studies have shown that the presence of even 10 ppm of sulfur-based contaminants, such as SO_2, H_2S, or COS, results in significant suppression of C_{2+} products in industry relevant GDE-based flow cells.[16−19] Therefore, cleaning the CO_2 feedstock is necessary to operate the CO_2R/COR electrolyzers continuously without losing C_{2+} selectivity and frequent catalyst regeneration or replacement.

Recent studies have also explored the tandem catalysis/two-step approach, where the first catalyst (typically Ag- or carbon-based) reduces CO_2 to CO and the product mixture of CO_2/CO is reduced to C_{2+} products on the second catalyst (typically Cu-based). A summary of experimental studies reporting current densities above 200 mA/cm^2 for CO_2R to CO in MEA and flow-based cells is shown in Table S3.[52−60] One of the major advantages of the two-step process is the possibility to minimize CO_2 loss to (bi)carbonate formation when acidic or neutral conditions are used. Studies have also reported reasonably high (>90%) FE toward CO under these conditions.[60−62] The conversion of CO_2 achieved in the first step is never 100%, and therefore a mixture of CO and hydrogen is obtained along with the unreacted CO_2. Depending on the conditions of the second step (acidic/neutral or alkaline), necessary purification of the feed mixture has to be performed to avoid reactant losses. The product distribution in a two-step system can also be controlled by changing the ratio of CO_2/CO fed to the second catalyst.[63−66]

Typical products obtained during CO_2R/COR on a copper catalyst include ethylene, acetate/acetic acid, ethanol, *n*-propanol, and hydrogen. Since acetic acid, ethanol, and propanol form a pinch point or an azeotrope with water, ordinary distillation would be impractical to separate these liquid products downstream in a cost-effective manner. Extractive distillation or pervaporation techniques have been proven to be effective in the separation of ethanol and water, while liquid−liquid extraction combined with azeotropic distillation can be used for the separation of acetic acid and water. Propanol can be separated either using extractive distillation or pervaporation

https://doi.org/10.1021/acs.iecr.5c03012
Ind. Eng. Chem. Res. 2026, 65, 1716−1733

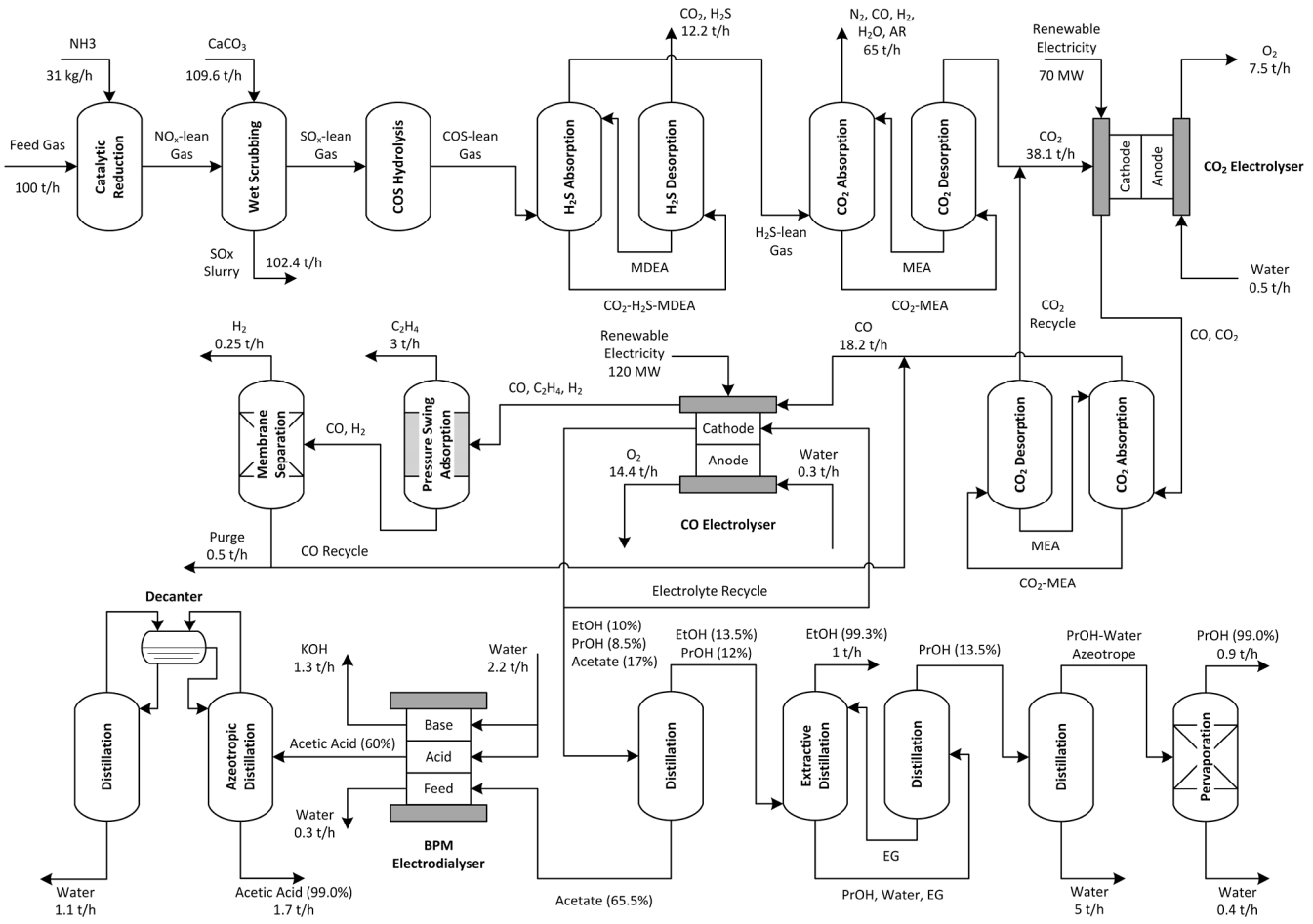

Figure 1. Overview of the two-step CO_2R/COR process utilizing a blast furnace gas (23% CO_2, 28% CO, 5% H_2, 40% N_2, 100 ppm of SO_2, 160 ppm of NO_x, 20 ppm of H_2S, and 20 ppm of COS) to produce C_{2+} products. The process includes the upstream gas cleaning units for the removal of impurities (NO_x, SO_2, H_2S, and COS), the CO_2R/COR electrolyzers, and the downstream product separation units for gases (H_2, C_2H_4) and liquids (ethanol, acetic acid, and *n*-propanol).

techniques after separating ethanol from the alcohol-rich stream.[67−69] Separation of gaseous components in the feed and product mixtures also involves certain challenges. For example, the separation of CO from N_2, which is typically present in feedstock from manufacturing industries, is difficult using conventional separation methods due to their similar kinetic diameters and boiling points.[70] Similarly, separation of ethylene from CO_2 using cryogenic distillation is impractical due to the formation of an azeotrope, while the separation of ethylene from CO becomes challenging due to their similar kinetic diameters and adsorption properties.[71] Hence, efficient and cost-effective separation strategies have to be identified to separate each component in the gas and liquid streams while ensuring the overall techno-economic feasibility of the CO_2R/COR plant.

It is evident that the successful large-scale implementation of the CO_2R requires a holistic approach that encompasses all stages of the process chain, from CO_2 capture to downstream product separation. Here, particular emphasis is placed on modeling the two-step CO_2R process, with a focus on incorporating an upstream cleaning process to remove harmful gaseous impurities. This integration is critical for maintaining the selectivity and stability of C_{2+} product formation, as impurities can severely impact the catalyst performance and overall process efficiency. Furthermore, the downstream separation of complex gaseous and liquid mixtures is crucial for achieving high product purity and economic feasibility. By integrating a detailed process model, including upstream gas cleaning and downstream product separation strategies, we aim to provide valuable insights into optimal technology selection for the commercialization of the CO_2R process.

3. PROCESS DESIGN AND MODELING

In this section, we present the process design and modeling of an integrated large-scale two-step CO_2R/COR plant that produces C_{2+} products including ethylene, acetic acid, ethanol, and *n*-propanol. This includes detailed modeling of the upstream gas cleaning units, CO_2 capture, electrochemical reduction of CO_2/CO, recycling of unreacted CO_2/CO, and downstream gas/liquid product separation. The entire CO_2R/COR plant is considered to be integrated with an existing steel manufacturing facility, where the byproduct gas generated in the plant, such as from the blast furnace, would be used as the feedstock for CO_2R. An integrated plant would typically require less costs compared to a standalone plant due to the availability of existing infrastructure, utilities, and storage, transportation, and distribution facilities within the plant. Hence, in this work, we assume that all the required units for the functioning of the CO_2R/COR plant are retrofitted into an existing plant.

https://doi.org/10.1021/acs.iecr.5c03012
Ind. Eng. Chem. Res. 2026, 65, 1716−1733

The blast furnace gas (BFG) stream typically comprises N_2 (40−50%), CO (25−30%), CO_2 (20−25%), H_2 (3−5%), and H_2O (2−3%) as the major components and minor components (<1%) such as Ar and O_2, on a mole basis.[72,73] However, trace amounts (<100 ppm mol) of contaminants such as NO_x, SO_x, H_2S, and COS are also typically present in BFG streams, which can potentially poison the CO_2R/COR catalysts and suppress the production of C_{2+} products. Hence, we design a process that utilizes 100 ton/h of BFG stream (typical capacity of a steel facility) comprising all the typical major, minor, and trace components for CO_2R/COR to produce C_{2+} products. The feed stream composition is assumed to be 40% N_2, 28% CO, and 23% CO_2 as major components and 160 ppm of NO_x, 100 ppm of SO_2, 20 ppm of H_2S, and 20 ppm of COS (by volume) as impurities (see Table S4), based on typical blast furnace gas compositions and the impurity data obtained from a steel mill. The BFG feedstock is assumed to be at a temperature of 150 °C and 1 bar. The effect of various contaminants on CO_2R/COR has been studied so far only by mixing one contaminant at a time with CO_2 gas, hence, we assume that a mixture of contaminants does not poison the CO_2R/COR catalysts as long as the concentration of each contaminant remains below its individual tolerance limit. The limits are assumed to be 5 ppm for NO_x and 1 ppm each for SO_2, H_2S, and COS, based on the recent experimental studies.[16−19] Since C_{2+} products such as ethylene, acetic acid, ethanol, and *n*-propanol typically account for the majority (>90%) of the COR products, it is assumed that with proper selection of catalyst and process design, the formation of minor products such as C_1 and C_3 can be minimized. Furthermore, we assume that H_2 and O_2 are the only gaseous byproducts formed in both the CO_2R/COR electrolyzers. The electrolyzers are assumed to be operated at ambient conditions (20 °C and 1 bar) with single pass conversions of 50% for CO_2 and 75% for CO in the first and second steps, respectively, based on similar modeling studies.[22,29] In the following sections, detailed modeling of the upstream, electrolyzers, and the downstream processes are presented. An overview of the overall CO_2R/COR plant utilizing industrial CO_2 feedstock to produce C_{2+} products is shown in Figure 1. The specifications and concentrations of all inlet/outlet streams are summarized in the supplementary excel file.

3.1. Process Design for Upstream Gas Cleaning

The gaseous contaminants that must be mainly removed from the feed stream for CO_2R/COR are NO_x, SO_x, COS, and H_2S. NO_x removal technologies are classified into oxidation, reduction, and adsorption/absorption approaches based on the valence of nitrogen.[74] Among these, selective catalytic reduction (SCR) of NO_x using ammonia (NH_3) has been widely used as a postcombustion de-NO_x strategy due to its high efficiency (>90%), good stability, and relatively lower temperatures (200−500 °C). Mn-based and V-based catalysts are widely used because of their highly selective NO_x removal potential. Since these catalysts are also resistant to poisoning to a good extent, SCR units can also be placed upstream to the SO_x removal units and in high dust positions.[74] The SCR unit is modeled as a stoichiometric reactor in Aspen Plus which operates at 350 °C and 1 bar, with a conversion efficiency of 96% for NO.[75] Since the NO_x mixture comprises ∼94% NO and only ∼6% NO_2, it is assumed that all of the NO_2 is reduced to N_2. An aqueous solution of 25% (w/w) NH_3 is used as the reducing agent. The reactions involved in the modeling of the SCR unit with their respective fractional conversions are summarized in Table S5. The SCR unit reduces the NO_x concentration in the BFG stream from ∼160 ppm to <5 ppm. Any particulate matter present in the BFG stream is also assumed to be removed in the electrostatic precipitator integrated with the SCR unit, which is not modeled explicitly in this work.

The NO_x-lean BFG stream is then sent to the desulfurization unit for the removal of SO_2 gas. Conventional SO_2 removal technologies include wet/dry scrubbing, catalytic oxidation/reduction, adsorption, absorption, and bioprocesses.[76,77] Among these, wet scrubbing using limestone has been widely used in industry due to its high removal efficiency (90−99%), reliability, low price of absorbents, and the possibility of converting SO_2 to solids for easy disposal. This process also consumes a high amount of energy and produces a large volume of slurry waste due to the fact that the absorbents cannot be recovered after the process. However, the calcium sulfite slurry obtained after the process can be converted into high-quality gypsum by forced oxidation, which then becomes a marketable byproduct.[76,77] The wet scrubbing unit is modeled in Aspen Plus as an absorber column (RADFRAC unit) with 6 stages operating at 1 bar, with the BFG entering at the bottom and the limestone slurry entering at the top. The ELECNRTL physical property method is used for the estimation of thermodynamic parameters of the electrolyte system. The number of moles of calcium carbonate in the lean slurry is calculated using a ratio of 1.04 per mole of SO_2 gas.[78,79] Table S6 summarizes the equilibrium and dissociation reactions involved in the modeling of the wet scrubbing unit. Almost complete removal of SO_2 is achieved using the wet scrubber from an initial concentration of ∼100 ppm, along with negligible amounts (1−2 ppm) of H_2S. The gypsum plant to valorize the calcium sulfite slurry is out of the scope of this work and hence not modeled.

There are several techniques to remove COS from industrial flue gas streams, including absorption, adsorption, hydrogenation, and hydrolysis. Due to the low energy consumption, relatively simple operation, and few side reactions, catalytic hydrolysis has been widely used for COS removal.[80] Catalysts for COS hydrolysis can be either unloaded or loaded with an active component such as alkali metals, transition metals, or rare metal oxides. Typical supports for loaded catalysts include γ-Al_2O_3, TiO_2, and activated carbon. Typically, the syngas is initially humidified in a water scrubber and then passed through a fixed-bed catalytic hydrolysis reactor operating at 175−205 °C, where over 99% of COS is converted to H_2S.[81] Since the BFG stream already contains around 2% water, which is much higher than the stoichiometric requirement (see Table S7) to convert ppm levels of COS, we directly feed the BFG to the reactor, modeled as an RSTOIC unit in Aspen Plus. Since the reaction is independent of the pressure, we assumed a pressure of 1 bar. The concentration of COS in the gas stream is reduced from ∼20 to ∼0.2 ppm in the reactor, while the concentration of H_2S is increased from ∼18 to ∼38 ppm.

Removal of H_2S from the BFG stream can be performed using various techniques such as absorption, adsorption, membrane separation, and biological processes. Among these, absorption of the acid gas into a liquid solvent has been an established technique since the 20th century.[82] Absorption can be classified as physical or chemical, depending on the type and strength of the interactions between the solvent and H_2S. Chemical absorption is characterized by strong interactions and is typically performed at low pressures, unlike physical absorption, which requires high pressures (>50 bar) and high H_2S partial pressures (>3 bar) for effective absorption. Chemical solvents can be

https://doi.org/10.1021/acs.iecr.5c03012
Ind. Eng. Chem. Res. 2026, 65, 1716−1733

recovered by using heat in a desorption column, while physical solvents require a pressure/temperature swing or air stripping for their recovery. Since the BFG is at 1 bar and the concentration of H_2S in the stream is very small (<40 ppm), chemical absorption would be the preferred choice in this case. Chemical absorption using alkanolamines is considered one of the most mature industrial technologies available for the sweetening of natural gas. Primary (e.g., monoethanolamine (MEA)) and secondary amines (e.g., diethanolamine (DEA)) have been known to be highly reactive toward both H_2S and CO_2; however, tertiary (e.g., methyldiethanolamine (MDEA)) and sterically hindered (e.g., aminomethyl propanol) amines have been known to be more selective toward H_2S.[83,84] Among these, MDEA is widely used despite its slightly higher cost due to several advantages. MDEA is more energy efficient with respect to solvent recovery due to its lower reaction enthalpy compared with MEA and DEA. MDEA is also more stable at elevated temperatures and less volatile, avoiding corrosion of the equipment and loss of the solvent via evaporation.[85] Hence, absorption using MDEA is chosen for the selective removal of H_2S in this work. The design parameters for the absorption and desorption columns (RADFRAC units) are summarized in Table S8.[86] All of the simulations regarding the absorber and desorber are performed using rate-based calculations and the ELECNRTL physical property method. The concentration of lean MDEA solvent used is 23.7% (w/w) in water.[86] The reactions used for the rate-based calculations are summarized in Table S9. Due to the coabsorption of CO_2 along with H_2S, around 12 ton/h CO_2 is also obtained from the desorber as a byproduct stream. Since this CO_2 stream contains ∼370 ppm of H_2S, which is much higher than the tolerable limit of 1 ppm for CO_2R/COR electrolyzers, utilization of this stream as a feedstock for CO_2R/COR is not possible. Therefore, this stream can only be utilized as a feedstock for alternate applications that can tolerate H_2S, or sent to a catalytic oxidation unit to convert all the H_2S to SO_2 and recycle the product stream back to the SO_2 scrubbing unit to recover the CO_2, which is out of the scope of this work. The lean MDEA solvent obtained from the bottom of the desorber column is recycled back to the absorber column, with only a negligible solvent makeup required. The H_2S-lean (∼0.3 ppm) BFG stream from the top of the absorber column is then sent to the CO_2 capture unit where CO_2 is separated from the rest of the BFG stream.

The need for CO_2 capture before the CO_2R electrolyzer is debatable since the stream is already clean enough to not poison the catalysts. However, since the cleaned stream contains around 42% N_2, 30% CO, 5% H_2, and 7% H_2O along with 16% CO_2, sending this stream directly to the electrolyzer will require a larger electrolyzer capacity to achieve the same conversion due to the lower partial pressure of CO_2. Moreover, if N_2 is let into the first electrolyzer, the separation of CO from the product stream containing N_2 will be another challenge due to their similar molecular properties such as kinetic diameters and boiling points.[70] Subsequently, N_2 will also reach the second electrolyzer, reducing the partial pressure of CO, thus again requiring a larger electrolyzer capacity. A majority of techno-economic studies suggest that electrolyzers contribute to 60−80% of the total CAPEX of a CO_2R/COR plant.[21−25,27,29] Thus, sizing-up the electrolyzers to accommodate the inert gases will lead to significant extra costs. On the other hand, separating the CO_2 stream from the rest of the BFG stream will make the electrolyzers smaller as well as the downstream product separation more convenient.

The CO_2 capture process is similar to the H_2S removal process, as typically both these gases are removed together as acid gases. Among the various technologies such as absorption, adsorption, and membrane separation, absorption using amine solvents is considered to be the most mature and cost-effective technology for postcombustion CO_2 capture.[87,88] For large-scale processes, the costs of CO_2 capture using membranes, pressure swing adsorption, and amine scrubbers are observed to be similar in the range of $25−50/ton CO_2.[89] We use a MEA solvent to capture CO_2 from the cleaned BFG stream due to the lower solvent cost and maturity of the technology. Table S10 summarizes the design parameters for the absorption and desorption columns modeled in Aspen Plus as RADFRAC units.[90,91] All of the simulations in the columns are performed using rate-based calculations and the ENRTL-RK physical property method. The concentration of lean MEA solvent used is 30% (w/w) in water. The reactions used for the rate-based calculations are summarized in Table S11. Around 21 tons/h of captured gas comprising CO_2 (95.1%) and CO (3.4%) is obtained from the top of the desorber column and can be utilized in the CO_2R electrolyzer. The lean MEA solvent obtained from the bottom of the desorber column is recycled back to the absorber column to reduce the operating costs. The unabsorbed gas from the top of the absorber column mainly contains ∼53.5% N_2, ∼36.5% CO, ∼7% H_2, and ∼2% H_2O and a lower heating value (LHV) of ∼4.57 GJ/h. This stream can be sent back to the steel mill to be burned as a low heating fuel or for electricity generation.

3.2. Process Design for CO_2R/COR Electrolyzers

In the two-step (CO_2R/COR) process, the first electrolyzer converts CO_2 to CO, which is further reduced to C_{2+} products in the second electrolyzer. The first electrolyzer can be either a low temperature electrolyzer or a high temperature solid-oxide electrochemical cell (SOEC). The SOEC process for CO production generally has a few advantages over the low temperature process, such as lower electric power consumption, higher CO_2 conversion, higher faradaic efficiency, higher cell stability, lower degradation rates, and a higher technology readiness level (TRL).[92] However, in this work, we focus on the low temperature electrolyzer, which operates at ambient conditions and has shown some significant progress recently, as summarized in Table S3. The first electrolyzer is assumed to operate in a zero-gap MEA (2-compartment) configuration and nonalkaline conditions to minimize the loss of CO_2 due to bicarbonate formation, with a FE of 96% for CO and 4% for H_2, at a current density of 500 mA/cm^2 and a cell voltage of 3 V.[29,55,66,93,94] Moreover, a conversion of 50% is assumed in the first electrolyzer, similar to other modeling studies.[29,95] The electrolyzer is modeled in Aspen Plus as a stoichiometric reactor (RSTOIC unit) operating at 20 °C and 1 bar. The calculations and reactions used to model the CO_2R electrolyzer are summarized in Section S5. We assume that there is no crossover of products across the membrane in the electrolyzer, which can be realized to an extent with the use of a cation exchange membrane. Since the FE for CO is less than 100%, a mixture of CO, unreacted CO_2, and small amounts of H_2 is obtained as products at the cathode side, while almost pure O_2 is obtained at the anode side. Studies have shown that the presence of CO_2 in the feed to the COR electrolyzer results in lower selectivity toward C_{2+} products and higher selectivity toward H_2 and C_1

https://doi.org/10.1021/acs.iecr.5c03012
Ind. Eng. Chem. Res. 2026, 65, 1716−1733

products.[65,66] Hence, to maximize C_{2+} product formation and to avoid formate or methane production, which would complicate the downstream processing, CO_2 capture is performed to separate CO_2 from the CO_2/CO product mixture.

The CO_2 capture unit after the first electrolyzer is modeled similarly as discussed earlier in the upstream cleaning section, where MEA solvent is used to absorb CO_2 from the gas mixture. Table S13 summarizes the design parameters for the absorption and desorption columns modeled in Aspen Plus. Around 17 tons/h of captured gas comprising ∼93.5% CO_2 and ∼5% CO is obtained from the top of the desorber column, which is recycled back to the first electrolyzer. The unabsorbed gas from the top of the absorber column mainly contains ∼94% CO, ∼4% H_2, and ∼2% H_2O (% mol), which is then directly fed to the second (COR) electrolyzer.

The second (COR) electrolyzer is operated in a hybrid MEA (with a cathode gas flow, a catholyte flow, and an anolyte flow) configuration and nonalkaline cathodic conditions. We assume that only ethylene, ethanol, *n*-propanol, acetic acid, and H_2 are produced in this electrolyzer with FEs of 50, 15, 15, 10, and 10%, respectively, similar to the study by Romero Cuellar et al.[66] For the base case, the electrolyzer is assumed to operate at 500 mA/cm^2 at a cell voltage of 2.5 V, but with a slightly higher conversion of 75% compared to the first electrolyzer, where the trend can be justified with experimental data.[29,46,66] The COR electrolyzer is also modeled in Aspen Plus as a stoichiometric reactor (RSTOIC unit), using calculated conversions based on FE of each product (see Section S7). It is again assumed that there is no crossover of products across the membrane in the second electrolyzer. A mixture of ethylene (∼36%), H_2 (∼28%), and unreacted CO (∼32%) is obtained as a gaseous product at the cathode side, which is then sent to the gas separation units, while almost pure O_2 is obtained at the anode side.

The concentration of liquid products (ethanol, acetic acid, and *n*-propanol) in the catholyte after a single pass through the electrolyzer is typically very low (<0.1 wt %) due to the large volume of electrolyte and the low FE toward liquid products. Downstream separation of liquid products from the electrolyte stream becomes energetically and economically infeasible if the concentrations of liquid products are not high enough.[96] Therefore, the catholyte stream is recycled back into the electrolyzer to undergo multiple passes, whereby the liquid products accumulate and the concentration increases. We have assumed a total recycle of catholyte until the liquid products reach an overall concentration of ∼35 wt %, which is high enough to justify the downstream operations. The number of passes required to achieve this concentration is calculated by extrapolating the concentration data from the first few passes, and this corresponds to approximately 1000 passes. Assuming an electrolyte storage capacity of three times that of the flow rate per minute to the electrolyzer (e.g., 3 L storage capacity for a flow rate of 1 L/min), it takes around 50 h (roughly 2 days) for the entire electrolyte to complete 1000 passes. Once the required concentration is achieved, 1 in 1000 parts of the electrolyte is extracted for downstream separation of the liquid products and an equivalent stream of fresh electrolyte is fed to the electrolyzer to make up for the extracted product stream. Electrolyte storage can also act as a buffer for downstream unit operations, such as distillation columns, which have challenging start-up or shut-down processes. This storage ensures an uninterrupted supply of liquid feed for up to 2 days, even if the electrolyzers need to be shut down for short maintenance periods. The electrolyte stream, after 1000 passes, has a concentration of ∼10 wt % ethanol, ∼17 wt % acetate/acetic acid, and ∼8 wt % *n*-propanol, which is then sent to the downstream units for the separation of liquid products. Furthermore, studies have shown that the swelling and performance degradation observed in Nafion membranes in the presence of higher organic concentrations (>10 wt %) can be prevented by incorporating matrix modifications with organic materials.[97,98] Therefore, we assume that the membrane performance remains unaffected by the liquid product concentration. In addition, we assume that the electrolyzer performance remains unaffected during the recycling of electrolyte as long as the electrolyte comprises at least 80 mol % (∼60 wt %) water.

3.3. Process Design for Downstream Product Separation

The gaseous product mixture obtained at the cathode side of the second electrolyzer mainly comprises CO (∼36%), ethylene (∼32%), and H_2 (∼28%) with minor amounts (∼2% each) of H_2O and Ar (from accumulation). Conventional technologies used in industries for the separation of CO from gas mixtures include cryogenic distillation, absorption, membrane separation, and adsorption.[99,100] However, separation of CO from a mixture containing ethylene is more challenging due to their similar kinetic diameters and adsorption/diffusion properties, as discussed earlier. Due to the very low selectivity of CO/ethylene, commercial membranes cannot be effectively used for their separation. Cryogenic distillation is not considered in this study due to its higher operating costs. Physical solvents such as Selexol and NMP could potentially be used to absorb ethylene out of the ethylene/CO mixture at higher pressures due to their relatively high ethylene/CO selectivity (∼10).[29,101] Studies have also focused on adsorption using expensive metal−organic frameworks (MOFs) and commercial zeolite adsorbents based on CaX and CuCl, for the separation of ethylene/CO with high selectivity.[102−104] In this work, we assume a five-bed vacuum pressure swing adsorption (VPSA) process using activated carbon as an adsorbent to separate ethylene from the mixture of CO and H_2. This separation is based on the numerical model developed by Xiao et al.,[105] incorporating mass and energy balances using a variety of adsorption isotherm, kinetic, and heat transfer models.[29] In this process, ethylene is recovered with a purity of at least 99%. The VPSA process operates at 25 °C and 10 bar feed pressure and mainly consists of adsorption, blow down, evacuation, and repressurization steps. In the first step, feed enters the bed at the bottom and the nonabsorbed gases leave at the top. The bed is then partially regenerated by venting the pressured column into the atmosphere. The bed pressure is further reduced in the next step using a vacuum pump to achieve higher bed regeneration, and in the last step, the bed pressure is increased to initial levels to start the next adsorption cycle. Typically, the purity/recovery increases with more steps, and the process becomes more cost-effective. The VPSA process is modeled in Aspen Plus as a separator (SEP-2) block that recovers 80% of the ethylene with a purity of 99% (remaining 1% being CO) (see Figure S8). With the development of better adsorbents that are more selective to ethylene, the separation efficiency of ethylene/CO could be further improved. Furthermore, the purity specifications for ethylene could vary depending on the type of application. For example, a polymerization process requires a purity >99.9%, while chemical grade or other applications can tolerate lower purities. Hence, further polishing steps might be needed after the VPSA to match

https://doi.org/10.1021/acs.iecr.5c03012
Ind. Eng. Chem. Res. 2026, 65, 1716−1733

the purity requirements per application, which are not included in this work.

The unabsorbed gas from the VPSA process comprises ∼9% ethylene, ∼38% H_2, and ∼49% CO and can be potentially used as a fuel within the plant. However, H_2 can be recovered from the stream and the remaining mixture of CO and ethylene can be recycled back into the second electrolyzer to increase the overall CO conversion. Separation of H_2 from flue gases is typically performed using techniques including cryogenic distillation, pressure swing adsorption (PSA), and membrane separation. Among these, membrane technology is widely used due to its low capital and operating costs, modularity, and ease of operation.[106] Polyimide-based membranes (Matrimid) have shown good thermal and chemical resistances along with a high free volume, providing high selectivity and permeability for H_2.[107,108] Studies have used the counter-current hollow fiber membrane model developed by Pettersen and Lien[109] to calculate the permeate mole fraction of components using design variables such as molar stage cut, pressure ratio, and dimensionless permeation factor.[29,110,111] In this work, we model the separation using a Matrimid/ZIF-8 polyimide membrane that operates at 80 °C and 10 bar of feed pressure. The membrane is modeled in Aspen Plus using a separator (SEP-2) block that recovers 92% of the H_2 with a purity of 99% at a permeate pressure of 1 bar. The calculations used to estimate the required membrane area for this separation are summarized in Section S8.[112] The retentate stream after the membrane separation contains ∼75% CO, ∼14% ethylene, and ∼5% H_2, which is then recycled back into the second (COR) electrolyzer after purging 10% of the stream to prevent accumulation of inert and impurity gases.

The catholyte stream from the COR electrolyzer, after accumulation of products, contains ∼10 wt % ethanol, ∼17 wt % acetate/acetic acid, and ∼8 wt % *n*-propanol. This stream is initially fed to a flash vessel to separate any dissolved gases, and the liquid stream obtained at the bottom of the vessel is fed to a distillation column to separate alcohols as the top product and acetate/acetic acid as the bottom product. The number of stages and the reflux ratio are optimized using the shortcut distillation column (DSTW unit) to minimize the capital and energy requirements for the distillation column. The parameters are then implemented in the rigorous distillation model (RADFRAC unit). The design parameters for the distillation column are summarized in Table S15. The simulations in the distillation column are performed by using equilibrium calculations and the NRTL physical property method. The alcohol stream obtained at the top of the column contains ∼13.5 wt % ethanol and ∼12% *n*-propanol, while the bottom stream contains ∼65% acetate/acetic acid as most of the water leaves at the top of the column.

Separation of ethanol and *n*-propanol in the alcohol stream is not straightforward, since both components form a low-boiling azeotrope with water. The azeotropic point of the ethanol/water system is 95.6 wt %, while *n*-propanol can be concentrated only up to 71.7 wt % by ordinary distillation. Furthermore, having a mixture of these components makes the separation of the two components even more complicated. Ethanol for application as a fuel requires a minimum purity of 99.5 wt % and this is typically achieved using methods such as azeotropic distillation, extractive distillation, adsorption using molecular sieves, and pervaporation. We will use extractive distillation with ethylene glycol as a solvent to break the azeotrope and separate ethanol from the mixture of *n*-propanol and water.[113,114] Almost pure ethanol (∼99.3 wt %) is obtained at the top of the distillation column, while a mixture of ethylene glycol, *n*-propanol, and water is obtained at the bottom. The bottom stream is then sent to a second distillation column, where almost pure ethylene glycol (∼99.99 wt %) is recovered as the bottom product, while *n*-propanol and water leave at the top of the column. Both the distillation columns are modeled in Aspen Plus using RADFRAC units and the design parameters for the distillation columns are summarized in Table S16. The simulations in the distillation columns are performed using equilibrium calculations and the NRTL physical property method. The distillate rates and the reflux ratios for both the columns are optimized to maximize the separation and minimize the energy requirements. The recovered ethylene glycol is then cooled and recycled back into the first (extractive) distillation column, with necessary makeup.

The dilute *n*-propanol (13.5 wt %) stream obtained at the top of the recovery column needs to be further dehydrated in order to meet at least the chemical grade specifications (>99.0 wt %). Due to the formation of an azeotrope, special distillation methods including azeotropic distillation, extractive distillation, and pressure swing distillation have been used for the dehydration of *n*-propanol.[115−117] Pervaporation (PV) is a relatively new membrane separation technology that separates components by using the chemical potential difference between the upstream and downstream components as the driving force. PV can be effectively used to separate near-boiling or azeotropic mixtures, as this technology is not limited by the relative volatility of the components. Due to the lower capacity and higher equipment cost of individual PV units, studies have explored combinations of traditional distillation with PV and have observed significant energy and cost savings.[67,118,119] Therefore, we use a traditional distillation column to concentrate the *n*-propanol stream close to its azeotropic point (71.7 wt %), followed by a series of PV units to further concentrate the *n*-propanol stream to above 99.0 wt %. The distillation column is modeled in Aspen Plus using a RADFRAC unit, and the simulations are performed using equilibrium calculations and the NRTL physical property method. The design parameters of the column are summarized in Table S17. Almost pure water (∼99.999 wt %) is obtained at the bottom of the distillation column, while a distillate stream with ∼67 wt % *n*-propanol is obtained at the top. This stream is fed to a series of PV units with a Sulzer PERVAP 1201 poly(vinyl alcohol) (PVA) composite flat-sheet membrane, each operating at a feed pressure of 3 bar, a permeate pressure of 3 mbar, and a feed temperature of 90 °C.[67] Each PV module is modeled in Aspen Plus using a separator (SEP-2) block. The design parameters and calculations for each module are summarized in Section S11. After seven PV modules (total module area of 420 m^2), the *n*-propanol concentration reaches ∼99.0 wt %, while the remaining 1 wt % is ethanol that is assumed to be retained in the retentate stream when water selectively permeates through the membrane. The permeate streams from all PV units, mainly containing water (>99.5 wt %), are combined, cooled, and brought to atmospheric pressure, before feeding it to the water treatment facility.

The bottom product obtained from the alcohol−acetate distillation column comprises ∼65 wt % acetate/acetic acid. Since the pH of the stream (∼6) is higher than the pK_a of acetic acid (4.76), the stream exists mainly in the conjugate base (deprotonated) form, i.e., as acetate ions. To obtain pure acetic acid as a product, acetate must be converted to acetic acid, which can then be further purified by using techniques such as

https://doi.org/10.1021/acs.iecr.5c03012
Ind. Eng. Chem. Res. 2026, 65, 1716−1733

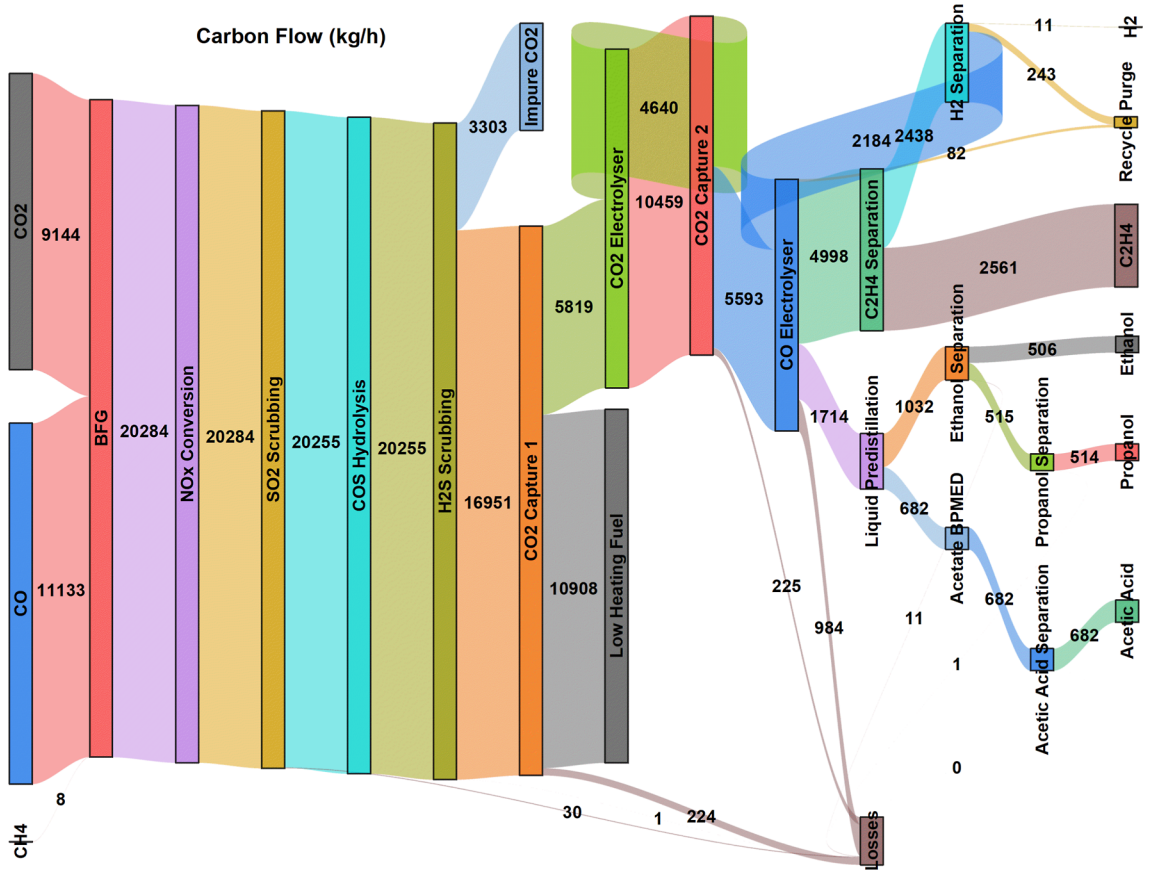

Figure 2. Carbon flow (kg/h) through every process unit in the integrated CO_2R/COR plant.

distillation. This can be done either by adding an acid to the stream to lower the pH below the pK_a of acetic acid or by electrodialysis (ED). The former method requires large amounts of acid and also dilutes the product stream further, while the latter method requires only water as feed to generate H^+/OH^- ions using electricity. We assume a bipolar membrane electrodialysis (BPMED) process with a membrane stack configuration of C-BP-A-C, where C is a cation exchange membrane (CEM), BP is a bipolar membrane (BPM), and A is an anion exchange membrane (AEM).[120,121] The acetate stream is fed to the first compartment (between A and C membranes), from which the acetate ions pass through the A membrane to the second (acid) compartment, where it combines with the H^+ ions supplied by the BP membrane to form acetic acid. The K^+ ions in the electrolyte stream pass through the C membrane to the electrode rinsing solution (K_2SO_4) that is circulated continuously around the outer compartments. These K^+ ions then pass through the C membrane on the other side of the electrodialyzer and reach the third (base) compartment, where it combines with the OH^- supplied by the BP membrane to form KOH. The ED process is assumed to operate at ambient conditions, a current density of 100 mA/cm^2, and a cell voltage of 5 V.[122] The size of the electrodialyzer is estimated assuming that all the acetate ions pass through the membrane and get converted to acetic acid, as summarized in Section S12. The ED process is modeled in Aspen Plus as a stoichiometric reactor (RSTOIC) followed by a separator (SEP-2) unit to separate the streams from the 3 compartments. The acetic acid obtained at the outlet of the acid compartment is mixed with the acetic acid stream obtained from the flash vessel before the ED and the final stream contains ~60 wt % acetic acid, which is further purified. The KOH stream obtained from the base compartment has a concentration of 3 M and can be utilized as anolyte in the second electrolyzer, with necessary dilution and/or makeup.

Dehydration of acetic acid using ordinary distillation is known to be energy and capital intensive due to the high reflux and number of stages required to obtain pure acetic acid. This can be attributed to the closeness in the volatility of acetic acid and water despite not forming an azeotrope. Separation techniques including multieffect distillation, heterogeneous azeotropic distillation, and hybrid extraction/distillation have been explored in various studies to compare the separation performance and total annual costs involved.[123−125] Among these, hybrid extraction/distillation has shown promising performances and cost savings. In this approach, the dilute (<30 wt %) acetic acid stream is initially concentrated using liquid−liquid extraction using solvents such as ethyl acetate (EA) or methyl *tert*-butyl ether (MTBE), and then the extracted phase (with acetic acid) is further concentrated using azeotropic distillation. Since the concentration of the acetic acid stream after the ED is much higher (~60 wt %), a liquid−liquid extraction step is not necessary in this case. We use azeotropic distillation with MTBE as a solvent due to its lower azeotropic point (52.6 °C) and density (740 kg/m^3) compared to EA (70.4 °C and 900 kg/m^3), which reduces the reboiler duty requirements and increases the separation efficiency of water and solvent phases. Almost pure acetic acid (~99.1 wt %) is obtained at the bottom of the distillation column, while an azeotropic mixture of MTBE and water is obtained at the top, which is then separated into aqueous and organic phases in a decanter. The aqueous phase

https://doi.org/10.1021/acs.iecr.5c03012
Ind. Eng. Chem. Res. 2026, 65, 1716−1733

from the decanter is fed to a stripping column, where almost pure water (~99.995 wt %) is obtained as the bottom product, while a lean mixture containing MTBE (~93.2 wt %) is obtained at the top which is recycled back into the decanter. The organic phase (lean solvent) from the decanter is recycled back into the azeotropic column with necessary makeup (negligible amount). Both the distillation columns are modeled in Aspen Plus using RADFRAC units and the design parameters for the distillation columns are summarized in Table S21. The simulations in the distillation columns are performed using equilibrium calculations and the NRTL-HOC physical property method where the binary interaction parameters used are based on the work of Li et al.[125] The bottom rate and reflux ratio of the dehydration column and the boil-up ratio of the stripping column are optimized to maximize the separation and minimize the energy requirements.

The carbon flow through every upstream, electrolyzer, and downstream process unit in the integrated CO_2R/COR plant is summarized in Figure 2.

The total amount of carbon in the BFG feed is ~20.3 ton/h, while the total amount of carbon that ends up in the final products (ethylene, ethanol, propanol, and acetic acid) is ~4.3 ton/h, which is ~21% of the BFG carbon. This is due to the fact that a major portion (~54% or ~10.9 ton/h) of the BFG carbon (in the form of CO) is separated out in the first CO_2 capture unit with a potential application as a low heating fuel in the steel mill. Among the total BFG carbon captured (~5.8 tons/h) in the first CO_2 capture unit, ~4.3 tons/h end up in the final products, suggesting a carbon conversion efficiency of 73.2%. The overall carbon losses in the process include ~3.3 ton/h (~16.3%) as impure CO_2 (from the H_2S scrubbing), ~0.3 ton/h (~1.6%) as recycle purge (mainly CO), and ~1.5 ton/h (~7.3%) as other general losses in the plant. The carbon utilization efficiency of the plant can be further improved by sending the impure CO_2 stream (from H_2S scrubbing) to a catalytic oxidation unit to convert all the H_2S to SO_2 using a part of the O_2 produced in the electrolyzers and recycling the product stream back to the SO_2 scrubbing unit. However, this is out of the scope of this work and hence not modeled.

4. ECONOMIC ANALYSIS OF THE CO_2R/COR PROCESS PLANT

Here, we present a detailed economic analysis of the integrated large-scale two-step CO_2R/COR plant including the upstream gas cleaning units, CO_2 capture, electrochemical reduction of CO_2/CO, recycling of unreacted CO_2/CO, and downstream gas/liquid product separation. The cost estimation of processes with limited literature data is performed by comparing them with closely related processes, for example, CO_2 electrolysis and water electrolysis. To account for the uncertainty in the estimation of the capital and operating costs of various plant components, a sensitivity analysis is performed on various operational and market parameters including electricity price, current density, cell voltage, electrolyzer cost, raw material price, and product price. Furthermore, better and worse case scenarios compared with the base case are provided to compare the relative impact of various parameters on the economics of the process.

4.1. Base Case Assumptions

The price of CO_2 feedstock depends on the source, concentration, and capture technology. This typically ranges between $25 and 50/ton for capture from large-scale industrial point sources and between $250 and 500/ton for direct capture from air.[126,127] As mentioned earlier, we assume the CO_2R/COR plant to be integrated with an existing steel manufacturing facility and the blast furnace gas generated in the facility can be used as the feedstock for the CO_2R/COR process. Since the 100 ton/h blast furnace gas (LHV ~3.04 GJ/ton) can be typically used within the steel mill as a low heating fuel or for electricity generation in a gas turbine, the utilization of BFG as a feed for the CO_2RR would cause a fuel energy deficit in the steel mill. This deficit can be minimized to an extent by supplying the ~65 ton/h of fuel gas stream (LHV ~4.57 GJ/ton) obtained from the top of the first CO_2 absorber column back to the steel mill, thus requiring only compensating for a net deficit of 6.32 GJ/h. The cost of natural gas for replacement is assumed to be $10/GJ.[128] The costs of MEA-based CO_2 capture after upstream BFG cleaning and after the first electrolyzer are estimated using the correlation of Bains et al.:[29,129]

$$\log_{10}[\text{cost}/(\$/\text{kg})] = -0.5558\log_{10}[\text{mole fraction of } CO_2] - 1.8462 \quad (1)$$

This correlation accounts for the CAPEX and the OPEX for different gas capture technologies including CO_2, excluding the costs of compression, transportation, and storage. To estimate the total annual costs ($/kg) for the capture process, we assume that 80% of the costs are due to OPEX and 20% due to CAPEX, based on the costs of mature CO_2 capture processes.[29,130] The CO_2 concentrations in the respective streams are used to estimate the capture costs. Moreover, we assume that no CO_2 is lost to bicarbonate formation in the electrolyzers and that it can be recovered and recycled back to the process. Additionally, we do not consider the effects of policies related to climate change or carbon tax/credits in our analysis.

Studies have shown that the electricity price plays a significant role in determining the economic feasibility of a power-to-X project such as CO_2R/COR due to the dominant operating costs.[21−25,27,29] Utilizing electricity generated from renewable energy sources such as wind and solar is necessary to render the process green; however, due to their intermittent nature, operating the plant continuously on these sources can be challenging. Due to the significant capital expenses of large-scale CO_2R/COR plants, operating the plant only during the period with low or negative electricity prices also becomes infeasible. Hence, a mix of electricity sources must be chosen in such a way that it is not highly carbon intensive and at the same time provides an uninterrupted supply of electricity. The wholesale electricity prices in Europe have been in the range of $40−50/MWh before the COVID-19 pandemic and decreased to around $20/MWh soon after the outbreak. However, the prices started to increase in the second half of 2021 beyond pre-COVID levels, while the war outbreak in Ukraine in the beginning of 2022 further accelerated this rise, leading to prices above $200/MWh. The electricity prices have been decreasing consistently since late 2022 and are expected to stabilize around the pre-COVID levels by the second half of 2024.[131−133] Therefore, we assume an electricity price of $40/MWh for the base case of the techno-economic analysis.

The capital and operating costs for SCR technology for NO_x reduction are estimated by sizing and indexing the costs based on a reference plant for coal-fired boilers (see Section S1).[134] The costs of the COS hydrolysis unit are estimated based on a reference unit installed in a syngas generation and conversion facility.[135] The costs of H_2S removal using MDEA are estimated

https://doi.org/10.1021/acs.iecr.5c03012
Ind. Eng. Chem. Res. 2026, 65, 1716−1733

similar to the CO_2 capture costs, using Bains'[129] correlation, as shown in Section S3. Since CO_2 is coabsorbed along with H_2S in the amine solvent, the system can be considered as a CO_2 capture unit where the initial concentration of CO_2 is calculated based on the amount of CO_2 coabsorbed in the process. The operating costs of the CO_2R/COR electrolyzers are estimated from the power consumption as

$$P_t = i_t A V \quad (2)$$

where P_t is the total power required by the electrolyzer, i_t is the total current density, A is the electrode area required, and V is the cell voltage. The electrode area (A) required for the CO_2R and COR electrolyzers is estimated in Sections S5 and S7, respectively. The capital costs of CO_2R/COR electrolyzers are estimated from other related electrolysis processes due to the absence of commercial-scale CO_2R/COR plants. Ramdin et al.[29] summarized the capital costs of various electrolysis processes including water electrolyzers (alkaline and SOEC), chlor-alkali processes, and aluminum smelters and estimated CO_2R/COR electrolyzer costs to be in the range of \$20,000/m^2 considering similar complexities and operating conditions of the processes. We assume similar electrolyzer capital costs for the base case and an annual maintenance cost of 2.5% of the capital cost.

The capital cost of the 5-bed VPSA process for ethylene separation is estimated using the guidelines provided by Luyben[136] (for compressors and pumps) and Woods[137] (for storage/pressure vessels, adsorbents, and valves). The operating cost of VPSA is estimated by using the power consumption of the compressors and vacuum pumps. The cost calculations of VPSA are summarized in Section S14. For the capital costs of membrane units for H_2 separation, a skid price of \$500/m^2 membrane area, including the cost of membrane modules, module housings, valves, instrumentation, piping, and frame structure, is assumed based on similar studies.[29,138,139] The required area for H_2 separation is estimated in Section S8. Additionally, the annual maintenance cost of membrane units is assumed to be 2.5% of the capital costs.[22] The capital and operating costs of the pervaporation units for *n*-propanol separation are estimated by sizing and indexing, based on the study by Wu et al. (see Section S11).[115] An estimation of capital cost for the BPMED unit for the conversion of acetate to acetic acid is performed using reference costs of \$1300/m^2 for the BP and \$145/m^2 for AE/CE membranes,[140] while the operation cost is estimated based on the power consumption (see Section S12). However, the capital and operating costs of all the distillation columns (for ethanol, *n*-propanol, and acetic acid separation), limestone wet-scrubbing column (for SO_2 removal), and the balance of plant (flash vessels, separation tanks, heat exchangers, pumps, compressors, etc.) are estimated using Aspen Plus. The pressure losses across process units and pipelines are neglected in this study to simplify the system-level modeling and focus on the dominant electrochemical and separation energy requirements. The utilities used in the process include cooling water (20 °C), low pressure steam (125 °C), medium pressure steam (175 °C), high pressure steam (250 °C), and refrigerant (−25 °C) at a cost of \$1.5/GJ, \$6/GJ, \$8/GJ, \$9/GJ, and \$8/GJ, respectively.[29] Furthermore, optimizing the heat exchanger network (HEN) to utilize process streams in the heat exchangers can save the utility costs by 30−50%.[141,142] Since performing a detailed HEN is out of the scope of this work, we assume the process achieves 40% utility cost savings with proper heat integration. The heat generated in the electrolyzers due to system inefficiency is also neglected in this work.

The cost of raw materials and the selling prices of products are assumed based on the European market and are summarized in Tables S24 and S25. Depending on the region and market conditions, these prices may vary significantly, therefore, the market conditions outside Europe are not considered for this study. Furthermore, the purity of products can also largely influence the selling prices. We assume that the products obtained from the CO_2R/COR process including ethylene (∼99.2%), ethanol (∼99.5 wt %), *n*-propanol (∼99.0 wt %), and acetic acid (∼99.1 wt %) meet the market standards after the purification steps. Moreover, the byproducts obtained including H_2 (∼99.2%) and O_2 (>99.9%) are also assumed to find suitable markets, especially since the demand for green hydrogen has been projected to grow significantly until 2050.[143,144]

To analyze the economic feasibility of the integrated CO_2R/COR process, we consider two cases: a base case and an optimistic case. The base case takes into account the current performance of electrolyzers, raw material costs, and product selling prices, whereas the optimistic case assumes the values of these parameters based on potential technology development and favorable market conditions in the future, as summarized in Table 1.

Table 1. Assumptions Made for the Large-Scale CO_2R/COR Process in the Two Cases

parameter	base case	optimistic case
feed flow rate (ton/h)	100	100
lifetime (years)	20	20
operating time (days/year)	350	350
electricity price (\$/MWh)	40	20
current density CO_2R (mA/cm^2)	500	750
current density COR (mA/cm^2)	500	750
cell voltage CO_2R (V)	3	2.5
cell voltage COR (V)	2.5	2
electrolyzer cost (\$/m^2)	20,000	10,000
raw material cost (%)	100%	100%
product selling price (%)	100%	135%

A feed (blast furnace gas) flow rate of 100 tons/h is considered for both cases to compare the effect of technology and market-related parameters on the economics of the plant. The plant is assumed to operate 350 days a year, with a downtime of 2 weeks for maintenance, over a 20 year lifetime. The electricity price is assumed to decrease from the current value of \$40/MWh to roughly \$20/MWh in the future with the increasing penetration of renewable energy sources such as wind and solar.[145,146] Moreover, several studies have already achieved current densities >750 mA/cm^2 for CO_2R/COR electrolyzers on laboratory scales (see Tables S1−S3); however, these are currently sustained only for a few hours (typically <10 h). It is assumed that with the development of technology, electrolyzers would be able to operate with a stability of at least 5000 h at current densities of 750 mA/cm^2, which is desirable for the commercialization of the CO_2R/COR. Similarly, the cell voltage of electrolyzers is assumed to be lower in the future with the improvements in catalysts, membranes, electrodes, electrolytes, and cell designs. The costs of electrolyzers are also expected to go down in the future if the components required for the electrolyzers are produced in large scales and also if the use of rare and expensive metals is avoided. The future market

https://doi.org/10.1021/acs.iecr.5c03012
Ind. Eng. Chem. Res. 2026, 65, 1716−1733

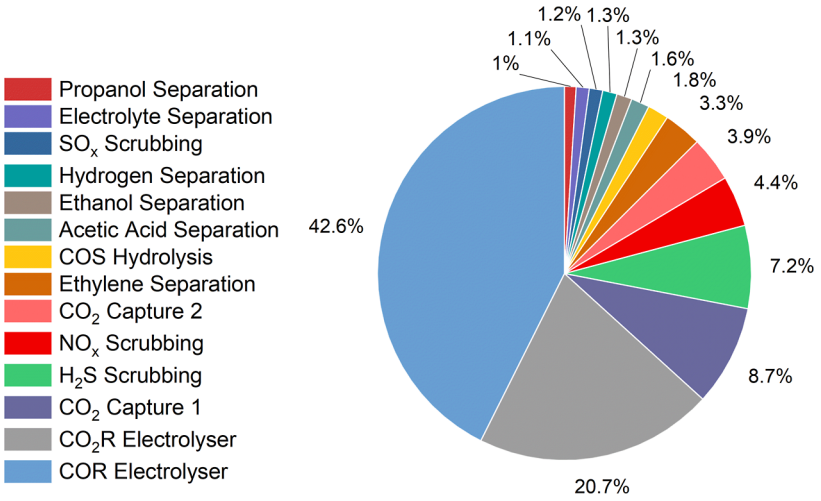

Figure 3. Total CAPEX ($452M) breakdown of the two-step CO_2R/COR process for the base case.

conditions are expected to be more favorable to sell the CO_2R/COR products such as ethylene, ethanol, *n*-propanol, and acetic acid, owing to the continuously increasing demand for these products. Therefore, a 35% increase in the product prices is assumed in the optimistic case.

4.2. Financial Assumptions

The return on investment for the large-scale CO_2R/COR plant is estimated based on the net present value (NPV) of the project over its 20 year lifetime. The construction of the plant is assumed to be completed in the first year, and the operation of the plant is assumed to begin from the second year. The initial working capital is assumed to be 5% of the capital investment and is recovered at the end of the project. A straight line depreciation is assumed over a period of 10 years by considering a salvage value of 10% of the total capital investment at the end of its lifetime. A nominal interest rate of 10% and an income tax rate of 25% are assumed for the calculations. The NPV is estimated using the following equation:

$$\mathrm{NPV} = \sum_{i=0}^{i=n} \frac{C_n}{(1+r)^n} \tag{3}$$

where C_0 is the initial capital investment (negative value), C_n is the cashflow in the *n*th year, and *r* is the interest rate. The capital cost of all individual units in the plant is combined to obtain the total CAPEX of the plant. The annual profit is estimated by subtracting the annual OPEX of the plant from the revenue generated by selling the products. The payback time is estimated by determining the year in which the cumulative present value becomes greater than or equal to zero, and the internal rate of return (IRR) is estimated by determining the interest rate that makes the NPV equal to zero.

4.3. Economic Analysis

The economic analysis of the large-scale CO_2R/COR process with upstream gas cleaning units and downstream gas/liquid product separation units is presented in this section (see the Supporting Information for detailed calculations). The capital and operating costs of all the process units and the revenue generated from selling the products for the base case are summarized in Tables S26 and S27. The total CAPEX and OPEX of the two-step CO_2R/COR plant for the base case are around $452M and $111M/year, respectively, and their corresponding breakdowns are shown in Figures 3 and 4. It is

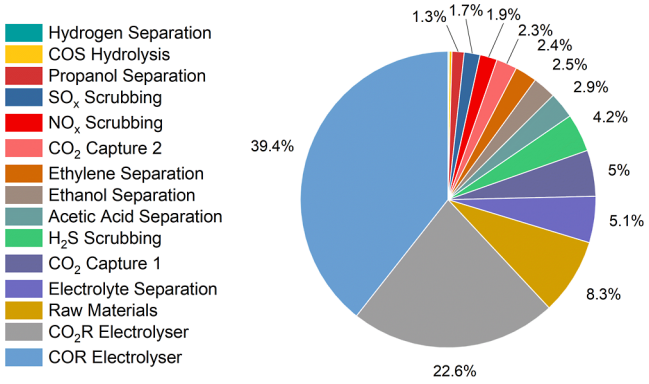

Figure 4. Total OPEX ($111M/y) breakdown of the two-step CO_2R/COR process for the base case.

interesting to note that the upstream cleaning units, including the two CO_2 capture units, contribute to only ~27% of the total CAPEX and ~15% of the total OPEX, while the electrolyzers alone contribute to ~63% of the total CAPEX and OPEX.

On the other hand, the downstream units, despite the difficult separation, only contribute to ~10% of the CAPEX and ~14% of the OPEX. The remaining ~8% of the OPEX is spent for the procurement of raw materials every year. The revenue generated from selling the products is around $84 million/year for the base case. The NPV calculated for the integrated two-step CO_2R/COR process is negative (−$692M) and the payback time is greater than the lifetime of the plant (>20 years). Therefore, the process is deemed to be economically unprofitable under the current best (base case) scenario. It is evident that the process cannot be profitable unless there is a significant development in technology to bring down the CAPEX and OPEX of the electrolyzers and the market conditions become more favorable to generate higher revenues from the products. Thus, future research should focus more on reducing the electrolyzer capital cost per area ($/m^2) and reducing the operational cell voltage required at higher current densities. Having lower electricity prices and higher product selling prices is also desirable to make the process profitable.

To better understand the effect of various capital, operational, and market parameters, a sensitivity analysis is performed on the electricity price, current density, cell voltage, electrolyzer cost, raw material price, and product price. A better and worse case is

https://doi.org/10.1021/acs.iecr.5c03012
Ind. Eng. Chem. Res. 2026, 65, 1716−1733

assumed for the sensitivity analysis by increasing or decreasing the base case parameters by 25%. The effect of each parameter on the NPV of the CO_2R/COR process is shown in Figure 5.

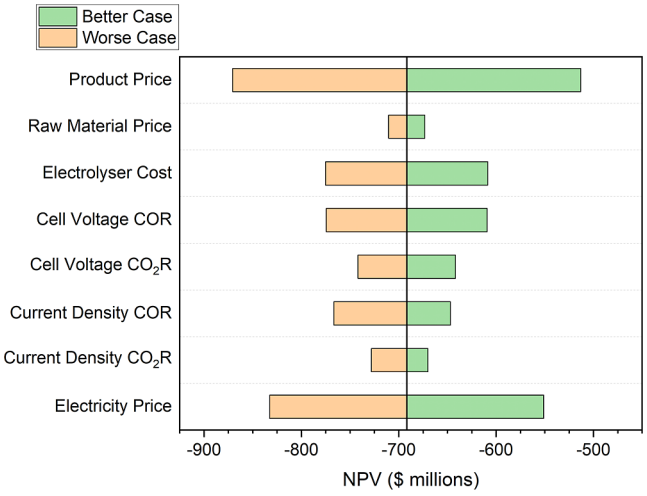

Figure 5. Sensitivity analysis of NPV for the two-step CO_2R/COR process with respect to various capital, operational, and market parameters. Base case parameters are summarized in Table 1. The better and worse cases are assumed by increasing or decreasing the values of the base case parameters by 25%.

The product price has the most influence on the NPV of the process, followed by the electricity price, whereas the raw material price has the least influence on the economics of the process. It is interesting to note that the cell voltage and the current density of the COR electrolyzer (second step) have more influence on the NPV than that of the CO_2R electrolyzer (first step). Thus, a positive NPV can be achieved only if a combination of major technological parameters is improved and the product selling price increases, as shown with the optimistic case (see Table 1).

The breakdown of CAPEX and OPEX of the two-step CO_2R/COR process and the revenue generated from selling the products for the optimistic case are shown in Tables S28 and S29. The total CAPEX and OPEX for the optimistic case are around \$261M and \$69M/year, respectively, while the revenue generation increases to \$113M/year. The NPV of the process becomes positive (\$54M) and a payback time of 13 years is achieved with an internal rate of return of 12.8%, which makes the process economically far more attractive.

The selectivity of the COR electrolyzer to produce specific C_{2+} products such as ethylene or ethanol is generally considered important for the economics of the process. However, by calculating the market value of products per mole of electrons consumed (V_e), the value of different products can be compared. This is summarized in Table 2 and is estimated as follows:[29]

$$V_e = P_p M_w / n \quad (4)$$

where V_e is the price of product per mole of electrons (\$/mol e^-), P_p is the market price of the product (\$/g), M_w is the molecular weight of the product (g/mol), and n is the number of moles of electrons required to produce 1 mol of product.

Among all the products obtained in the CO_2R/COR process, acetic acid has the highest value at $\$5.33 \times 10^{-3}$/mol of electrons, followed by green hydrogen ($\$4.95 \times 10^{-3}$/mol of electrons), n-propanol ($\$4.44 \times 10^{-3}$/mol of electrons), ethanol ($\$4.15 \times 10^{-3}$/mol of electrons), and ethylene ($\$2.92 \times 10^{-3}$/mol of electrons). Oxygen has the least value at $\$0.30 \times 10^{-3}$/mol of electrons; however, since oxygen is produced at the anode side as part of the overall reaction in the electrolyzer, it can be considered as an extra income. It is interesting to note that C_{2+} liquid products such as ethanol, n-propanol, and acetic acid have a higher value per mole of electrons compared to ethylene, suggesting that the economics of the process will only be impacted positively with a higher selectivity toward C_{2+} liquid products. Moreover, the value per electron mole of hydrogen byproduct is also higher than that of ethylene considering the current market conditions. This can be attributed to the fact that green hydrogen has a higher market price (\$3−\$8/kg) due to increased production costs compared to the relatively cheaper gray hydrogen produced from fossil fuels (\$1−\$2/kg).[153,154] Furthermore, since downstream separation of products contributes to only ∼10% of the CAPEX and ∼14% of the OPEX of the entire plant, producing multiple high value products will only have a positive impact on the process economics. Previous studies have drawn different conclusions favoring the production of ethylene due to the difference in the prices of components or due to the assumption of only limited products (mainly hydrogen and ethylene) for their analyses.[21,22,24,25,29] It is worth noting that despite having a series of upstream cleaning units to separate the gaseous impurities from the CO_2 feedstock, their contributions to the total CAPEX and OPEX are only ∼15% and ∼8%, respectively. In contrast, the two CO_2 capture units alone contribute to ∼13% of the CAPEX and ∼7% of the OPEX. Thus, commercialization of cheaper CO_2 capture alternatives including adsorption and membrane separation for similar gaseous mixtures needs to be further studied. Nevertheless, it is evident that the major focus should be on reducing the cost of electrolyzers (CAPEX and OPEX ∼ 63%), especially in terms of lowering the operational voltage, improving the current density, and improving the selectivity toward higher value products in order to bring the CO_2R/COR process closer to large-scale implementation.

Table 2. Price of Different Products (as of May 2024) per Mole of Electrons Required to Produce Them from CO_2

product	n (e/mol)	M_w (g/mol)	price (\$/ton)	$V_e \times 1000$ (\$/e)
ethylene	12	28.05	1,250[147]	2.92
ethanol	12	46.07	1,080[148]	4.15
n-propanol	18	60.09	1,330[149]	4.44
acetic acid	8	60.05	710[150]	5.33
green hydrogen	2	2.016	4,910[151]	4.95
oxygen	4	15.99	75[152]	0.30

Multiple studies have previously analyzed the economics of the two-step CO_2R/COR process incorporating the SOEC process as the first step and concluded that it can be economically even more attractive compared to the low temperature CO_2R process due to the maturity of the technology and lower costs involved.[24,29,155−157] However, even in such high temperature systems, the presence of gaseous contaminants can prove to be detrimental to the catalysts and will require dedicated upstream cleaning units for the continuous production of high value C_{2+} products. Other studies have also explored the process of coelectrolysis where, along with the CO_2 reduction at the cathode side, an oxidation reaction is also carried out at the anode side to produce a more valuable product than oxygen. Co-electrolysis of CO_2 to CO and glycerol to glycolic acid or formate has been studied recently and

https://doi.org/10.1021/acs.iecr.5c03012
Ind. Eng. Chem. Res. 2026, 65, 1716−1733

proved to be highly efficient, with energy savings of up to 80%.[158−160] However, these coelectrolysis processes also introduce some additional challenges such as the optimization of the reactions on both the sides, prevention of product crossover, selection of compatible membranes, separation and recovery of products, etc.[29] Furthermore, integration of the CO_2R/COR plant with gas-to-liquid or power-to-liquid facilities, where the products can be directly utilized, can significantly reduce the downstream costs and improve the economics of the plant.[161] These can include processes such as the production of ethylene oxide, vinyl acetate, and synthetic crude, where the CO_2R/COR products can be directly upgraded to more valuable chemicals or fuels.

5. CONCLUSIONS

We present a comprehensive process model and techno-economic analysis of an integrated large-scale two-step CO_2/CO electroreduction plant that produces C_{2+} products including ethylene, acetic acid, ethanol, and *n*-propanol, using blast furnace gas obtained from an integrated steel manufacturing facility as feedstock. Dedicated upstream gas cleaning units are modeled in order to remove the gaseous contaminants present in the industry-supplied CO_2 feedstock, such as SO_2, NO_x, COS, and H_2S, which can poison the silver and copper catalysts in the CO_2R/COR electrolyzers. The removal of these contaminants ensures a high selectivity toward C_{2+} products and reduces the operational costs associated with catalyst regeneration or replacement. Modeling of the CO_2 capture units, CO_2R/COR electrolyzers, recycling of unreacted CO_2/CO, and downstream separation of gas (ethylene, H_2, and CO) and liquid (ethanol, *n*-propanol, and acetic acid) products is also performed in detail using Aspen Plus to analyze the impact of different units on the overall economics of the large-scale CO_2R/COR plant.

Our techno-economic analysis shows that the large-scale two-step CO_2R/COR process is economically unfeasible with the current performance of electrolyzers (cell voltage and current density), electricity prices, product selling prices, and electrolyzer capital costs. The contribution of electrolyzers toward the total CAPEX and OPEX is the largest (∼63%), while the downstream units contribute to only ∼10% of the CAPEX and ∼14% of the OPEX. The NPV for the base case (current best scenario) is negative at −$692 M and the project never pays back. However, the process achieves a positive NPV ($54M), a payback time of 13 years, and an IRR of 12.8% when the electrolyzer capital cost reduces to $10,000/m^2, with an electricity price of $20/MWh, current density of 750 mA/cm^2 for both electrolyzers, and cell voltages of 2.5 V for CO_2R and 2.0 V for COR electrolyzers, and when the product prices are 35% higher. This shows that the process can be economically feasible only with significant improvements in electrolyzer design and performance (better catalysts, cell designs, membranes, etc.) and favorable market conditions. We also show that C_{2+} liquid products acetic acid, *n*-propanol, and ethanol possess higher value per mole of electron compared to ethylene, and therefore their production will only have a positive impact on the economics, considering that the downstream separation costs are relatively lower. This also emphasizes the need for upstream gas cleaning as the contaminants will otherwise suppress the production of high value C_{2+} products. Future studies should focus more on reducing the capital and energy costs by incorporating more mature and less expensive SOEC processes or energy saving coelectrolysis into the two-step CO_2R/COR process. Integrating the CO_2R/COR plant with facilities that can directly utilize the gas/liquid products can also significantly reduce the costs related to the downstream separation, storage, transportation, and distribution of products.

Overall, our techno-economic analysis revealed several key insights into the operational parameters and economic feasibility of the two-step low temperature CO_2R/COR process. By identifying potential bottlenecks and areas for improvement, our study provides valuable guidance for future research and development efforts aimed at the commercialization of the CO_2R process. The integration of our CO_2R/COR plant with an existing manufacturing facility, such as a steel plant, highlights the potential for utilizing industrial byproduct gas as a feedstock, further enhancing the economic and environmental benefits of this technology.

■ ASSOCIATED CONTENT

Supporting Information

The Supporting Information is available free of charge at https://pubs.acs.org/doi/10.1021/acs.iecr.5c03012.

Summary of studies performing electrolysis of CO_2 to CO, CO_2 to C_{2+} products, and CO to C_{2+} products; details of modeling of the SCR process, limestone wet scrubbing process, COS hydrolysis process, H_2S absorption process, CO_2 capture process, CO_2R/COR electrolyzers, membrane separation process, VPSA, traditional/extractive/azeotropic distillation processes, pervaporation process, and electrodialyzer; and summary of cost estimation and parameters (PDF)

Techno-economic analysis calculations for all units and stream summaries (XLSX)

■ AUTHOR INFORMATION

Corresponding Author

Mahinder Ramdin − *Department of Process & Energy, Faculty of Mechanical Engineering, Delft University of Technology, 2628 CB Delft, The Netherlands;* orcid.org/0000-0002-8476-7035; Email: m.ramdin@tudelft.nl

Authors

Asvin Sajeev − *Department of Process & Energy, Faculty of Mechanical Engineering, Delft University of Technology, 2628 CB Delft, The Netherlands;* orcid.org/0000-0001-6791-7292

Matthijs Kroes − *Department of Chemical Engineering, Faculty of Applied Sciences, Delft University of Technology, 2629 HZ Delft, The Netherlands*

Isabell Bagemihl − *Department of Chemical Engineering, Faculty of Applied Sciences, Delft University of Technology, 2629 HZ Delft, The Netherlands*

Ruud Kortlever − *Department of Process & Energy, Faculty of Mechanical Engineering, Delft University of Technology, 2628 CB Delft, The Netherlands;* orcid.org/0000-0001-9412-7480

Wiebren de Jong − *Department of Process & Energy, Faculty of Mechanical Engineering, Delft University of Technology, 2628 CB Delft, The Netherlands*

Complete contact information is available at: https://pubs.acs.org/10.1021/acs.iecr.5c03012

Author Contributions

Asvin Sajeev: Conceptualization, methodology, investigation, writing—original draft, and writing—review and editing. Matthijs Kroes and Isabell Bagemihl: Conceptualization, investigation, and writing—review and editing. Ruud Kortlever and Wiebren de Jong: Funding acquisition, supervision, and writing—review and editing. Mahinder Ramdin: Supervision and writing—review and editing.

Notes

The authors declare no competing financial interest.

■ ACKNOWLEDGMENTS

This study is part of the "Reactor, Process and System Design" project of the E2CB consortium, which is financed by NWO via the Perspective programme and affiliated industrial partners under the project number P17-08. The authors would also like to thank Advait Natu for his preliminary work on gas cleaning and separation.

■ REFERENCES

(1) Liang, S.; Altaf, N.; Huang, L.; Gao, Y.; Wang, Q. Electrolytic Cell Design for Electrochemical CO2 Reduction. *J. CO2 Util.* **2020**, *35*, 90−105.

(2) Kondratenko, E. V.; Mul, G.; Baltrusaitis, J.; Larrazábal, G. O.; Pérez-Ramírez, J. Status and Perspectives of CO2 Conversion into Fuels and Chemicals by Catalytic, Photocatalytic and Electrocatalytic Processes. *Energy Environ. Sci.* **2013**, *6*, 3112−3135.

(3) Nitopi, S.; Bertheussen, E.; Scott, S. B.; Liu, X.; Engstfeld, A. K.; Horch, S.; Seger, B.; Stephens, I. E. L.; Chan, K.; Hahn, C.; Nørskov, J. K.; Jaramillo, T. F.; Chorkendorff, I. Progress and Perspectives of Electrochemical CO2 Reduction on Copper in Aqueous Electrolyte. *Chem. Rev.* **2019**, *119*, 7610−7672.

(4) Spinner, N. S.; Vega, J. A.; Mustain, W. E. Recent Progress in the Electrochemical Conversion and Utilization of CO2. *Catal. Sci. Technol.* **2012**, *2*, 19−28.

(5) Garza, A. J.; Bell, A. T.; Head-Gordon, M. Mechanism of CO2 Reduction at Copper Surfaces: Pathways to C2 Products. *ACS Catal.* **2018**, *8*, 1490−1499.

(6) Kortlever, R.; Shen, J.; Schouten, K. J. P.; Calle-Vallejo, F.; Koper, M. T. M. Catalysts and Reaction Pathways for the Electrochemical Reduction of Carbon Dioxide. *J. Phys. Chem. Lett.* **2015**, *6*, 4073−4082.

(7) Whipple, D. T.; Kenis, P. J. A. Prospects of CO2 Utilization via Direct Heterogeneous Electrochemical Reduction. *J. Phys. Chem. Lett.* **2010**, *1*, 3451−3458.

(8) Lawrence, K. R.; Kumar, A. S.; Asperti, S.; van den Berg, D.; Girichandran, N.; Kortlever, R. Advances in Electrochemical Carbon Dioxide Reduction Toward Multi-Carbon Products. In *Chemical Valorisation of Carbon Dioxide*; Stefanidis, G., Stankiewicz, A., Eds.; The Royal Society of Chemistry: London, 2022; pp 388−412.

(9) Lum, Y.; Yue, B.; Lobaccaro, P.; Bell, A. T.; Ager, J. W. Optimizing C-C Coupling on Oxide-Derived Copper Catalysts for Electrochemical CO2 Reduction. *J. Phys. Chem. C* **2017**, *121*, 14191−14203.

(10) Philips, M. F.; Gruter, G.-J. M.; Koper, M. T. M.; Schouten, K. J. P. Optimizing the Electrochemical Reduction of CO 2 to Formate: A State-of-the-Art Analysis. *ACS Sustain. Chem. Eng.* **2020**, *8*, 15430−15444.

(11) Li, Y.; Sun, Q. Recent Advances in Breaking Scaling Relations for Effective Electrochemical Conversion of CO 2. *Adv. Energy Mater.* **2016**, *6*, 1600463.

(12) Luc, W.; Rosen, J.; Jiao, F. An Ir-Based Anode for a Practical CO2 Electrolyzer. *Catal. Today* **2017**, *288*, 79−84.

(13) Dufek, E. J.; Lister, T. E.; McIlwain, M. E. Bench-Scale Electrochemical System for Generation of CO and Syn-Gas. *J. Appl. Electrochem.* **2011**, *41*, 623−631.

(14) D'Alessandro, D. M.; Smit, B.; Long, J. R. Carbon Dioxide Capture: Prospects for New Materials. *Angew. Chem., Int. Ed.* **2010**, *49*, 6058−6082.

(15) Metz, B.; Davidson, O.; de Coninck, H.; Loos, M.; Meyer, L. *IPCC Special Report on Carbon Dioxide Capture and Storage*; IPCC: Cambridge, UK, 2005. https://www.ipcc.ch/report/carbon-dioxide-capture-and-storage/ (accessed 2023−03−29.

(16) Zhai, Y.; Chiachiarelli, L.; Sridhar, N. Effect of Gaseous Impurities on the Electrochemical Reduction of CO 2 on Copper Electrodes. *ECS Trans.* **2009**, *19*, 1−13.

(17) Luc, W.; Ko, B. H.; Kattel, S.; Li, S.; Su, D.; Chen, J. G.; Jiao, F. SO 2 -Induced Selectivity Change in CO 2 Electroreduction. *J. Am. Chem. Soc.* **2019**, *141*, 9902−9909.

(18) Ko, B. H.; Hasa, B.; Shin, H.; Jeng, E.; Overa, S.; Chen, W.; Jiao, F. The Impact of Nitrogen Oxides on Electrochemical Carbon Dioxide Reduction. *Nat. Commun.* **2020**, *11*, 1−9.

(19) Harmon, N. J.; Wang, H. Electrochemical CO2 Reduction in the Presence of Impurities: Influences and Mitigation Strategies. *Angew. Chem., Int. Ed.* **2022**, *61*, No. e202213782.

(20) Papangelakis, P.; Miao, R. K.; Lu, R.; Liu, H.; Wang, X.; Ozden, A.; Liu, S.; Sun, N.; O'Brien, C. P.; Hu, Y.; Shakouri, M.; Xiao, Q.; Li, M.; Khatir, B.; Huang, J. E.; Wang, Y.; Xiao, Y. C.; Li, F.; Zeraati, A. S.; Zhang, Q.; Liu, P.; Golovin, K.; Howe, J. Y.; Liang, H.; Wang, Z.; Li, J.; Sargent, E. H.; Sinton, D. Improving the SO2 Tolerance of CO2 Reduction Electrocatalysts Using a Polymer/Catalyst/Ionomer Heterojunction Design. *Nat. Energy* **2024**, *9*, 1011−1020.

(21) Detz, R. J.; Ferchaud, C. J.; Kalkman, A. J.; Kemper, J.; Sánchez-Martínez, C.; Saric, M.; Shinde, M. V. Electrochemical CO 2 Conversion Technologies: State-of-the-Art and Future Perspectives. *Sustainable Energy Fuels* **2023**, *7*, 5445−5472.

(22) Jouny, M.; Luc, W.; Jiao, F. General Techno-Economic Analysis of CO2 Electrolysis Systems. *Ind. Eng. Chem. Res.* **2018**, *57*, 2165−2177.

(23) Spurgeon, J. M.; Kumar, B. A Comparative Technoeconomic Analysis of Pathways for Commercial Electrochemical CO2 Reduction to Liquid Products. *Energy Environ. Sci.* **2018**, *11*, 1536−1551.

(24) Sisler, J.; Khan, S.; Ip, A. H.; Schreiber, M. W.; Jaffer, S. A.; Bobicki, E. R.; Dinh, C. T.; Sargent, E. H. Ethylene Electrosynthesis: A Comparative Techno-Economic Analysis of Alkaline vs Membrane Electrode Assembly vs CO2-CO-C2H4Tandems. *ACS Energy Lett.* **2021**, *6*, 997−1002.

(25) Somoza-Tornos, A.; Guerra, O. J.; Crow, A. M.; Smith, W. A.; Hodge, B.-M. Process Modeling, Techno-Economic Assessment, and Life Cycle Assessment of the Electrochemical Reduction of CO2: A Review. *iScience* **2021**, *24*, 102813.

(26) Na, J.; Seo, B.; Kim, J.; Lee, C. W.; Lee, H.; Hwang, Y. J.; Min, B. K.; Lee, D. K.; Oh, H.-S.; Lee, U. General Technoeconomic Analysis for Electrochemical Coproduction Coupling Carbon Dioxide Reduction with Organic Oxidation. *Nat. Commun.* **2019**, *10*, 1−13.

(27) Shin, H.; Hansen, K. U.; Jiao, F. Techno-Economic Assessment of Low-Temperature Carbon Dioxide Electrolysis. *Nat. Sustain* **2021**, *4*, 911−919.

(28) Orella, M. J.; Brown, S. M.; Leonard, M. E.; Román-Leshkov, Y.; Brushett, F. R. A General Technoeconomic Model for Evaluating Emerging Electrolytic Processes. *Energy Technol.* **2020**, *8*, 1900994.

(29) Ramdin, M.; De Mot, B.; Morrison, A. R. T.; Breugelmans, T.; van den Broeke, L. J. P.; Trusler, J. P. M.; Kortlever, R.; de Jong, W.; Moultos, O. A.; Xiao, P.; Webley, P. A.; Vlugt, T. J. H. Electroreduction of CO2/CO to C2 Products: Process Modeling, Downstream Separation, System Integration, and Economic Analysis. *Ind. Eng. Chem. Res.* **2021**, *60*, 17862−17880.

(30) Barcelos, M. M.; Vasconcellos, M. de L. S.; Ribeiro, J. Recent Progress in Electrochemical CO2 Reduction at Different Electrocatalyst Materials. *Processes* **2024**, *12*, 303.

(31) Zhu, D. D.; Liu, J. L.; Qiao, S. Z. Recent Advances in Inorganic Heterogeneous Electrocatalysts for Reduction of Carbon Dioxide. *Adv. Mater.* **2016**, *28*, 3423−3452.

https://doi.org/10.1021/acs.iecr.5c03012
Ind. Eng. Chem. Res. 2026, 65, 1716−1733

(32) Long, C.; Li, X.; Guo, J.; Shi, Y.; Liu, S.; Tang, Z. Electrochemical Reduction of CO2 over Heterogeneous Catalysts in Aqueous Solution: Recent Progress and Perspectives. *Small Methods* **2019**, *3*, 1800369.
(33) Sánchez-Sánchez, C. M.; Montiel, V.; Tryk, D. A.; Aldaz, A.; Fujishima, A. Electrochemical Approaches to Alleviation of the Problem of Carbon Dioxide Accumulation. *Pure Appl. Chem.* **2001**, *73*, 1917−1927.
(34) Kuhl, K. P.; Cave, E. R.; Abram, D. N.; Jaramillo, T. F. New Insights into the Electrochemical Reduction of Carbon Dioxide on Metallic Copper Surfaces. *Energy Environ. Sci.* **2012**, *5*, 7050−7059.
(35) Jitaru, M.; Lowy, D. A.; Toma, M.; Toma, B. C.; Oniciu, L. Electrochemical Reduction of Carbon Dioxide on Flat Metallic Cathodes. *J. Appl. Electrochem.* **1997**, *27*, 875−889.
(36) Inoue, A.; Harada, T.; Nakanishi, S.; Kamiya, K. Ultra-High-Rate CO2 Reduction Reactions to Multicarbon Products with a Current Density of 1.7 A Cm −2 in Neutral Electrolytes. *EES Catal.* **2023**, *1*, 9−16.
(37) Zheng, M.; Wang, P.; Zhi, X.; Yang, K.; Jiao, Y.; Duan, J.; Zheng, Y.; Qiao, S.-Z. Electrocatalytic CO2-to-C2+ with Ampere-Level Current on Heteroatom-Engineered Copper via Tuning *CO Intermediate Coverage. *J. Am. Chem. Soc.* **2022**, *144*, 14936−14944.
(38) García de Arquer, F. P.; Dinh, C.-T.; Ozden, A.; Wicks, J.; McCallum, C.; Kirmani, A. R.; Nam, D.-H.; Gabardo, C.; Seifitokaldani, A.; Wang, X.; Li, Y. C.; Li, F.; Edwards, J.; Richter, L. J.; Thorpe, S. J.; Sinton, D.; Sargent, E. H. CO 2 Electrolysis to Multicarbon Products at Activities Greater than 1 A Cm −2. *Science* **2020**, *367*, 661−666.
(39) Dinh, C.-T.; Burdyny, T.; Kibria, M. G.; Seifitokaldani, A.; Gabardo, C. M.; García de Arquer, F. P.; Kiani, A.; Edwards, J. P.; De Luna, P.; Bushuyev, O. S.; Zou, C.; Quintero-Bermudez, R.; Pang, Y.; Sinton, D.; Sargent, E. H. CO2 Electroreduction to Ethylene via Hydroxide-Mediated Copper Catalysis at an Abrupt Interface. *Science* **2018**, *360*, 783−787.
(40) Hoang, T. T. H.; Verma, S.; Ma, S.; Fister, T. T.; Timoshenko, J.; Frenkel, A. I.; Kenis, P. J. A.; Gewirth, A. A. Nanoporous Copper-Silver Alloys by Additive-Controlled Electrodeposition for the Selective Electroreduction of CO 2 to Ethylene and Ethanol. *J. Am. Chem. Soc.* **2018**, *140*, 5791−5797.
(41) Wang, X.; Wang, Z.; García de Arquer, F. P.; Dinh, C.-T.; Ozden, A.; Li, Y. C.; Nam, D.-H.; Li, J.; Liu, Y.-S.; Wicks, J.; Chen, Z.; Chi, M.; Chen, B.; Wang, Y.; Tam, J.; Howe, J. Y.; Proppe, A.; Todorović, P.; Li, F.; Zhuang, T.-T.; Gabardo, C. M.; Kirmani, A. R.; McCallum, C.; Hung, S.-F.; Lum, Y.; Luo, M.; Min, Y.; Xu, A.; O'Brien, C. P.; Stephen, B.; Sun, B.; Ip, A. H.; Richter, L. J.; Kelley, S. O.; Sinton, D.; Sargent, E. H. Efficient Electrically Powered CO2-to-Ethanol via Suppression of Deoxygenation. *Nat. Energy* **2020**, *5*, 478−486.
(42) Ozden, A.; Li, F.; Garcıa de Arquer, F. P.; Rosas-Hernández, A.; Thevenon, A.; Wang, Y.; Hung, S.-F.; Wang, X.; Chen, B.; Li, J.; Wicks, J.; Luo, M.; Wang, Z.; Agapie, T.; Peters, J. C.; Sargent, E. H.; Sinton, D. High-Rate and Efficient Ethylene Electrosynthesis Using a Catalyst/Promoter/Transport Layer. *ACS Energy Lett.* **2020**, *5*, 2811−2818.
(43) Wang, Y.; Wang, Z.; Dinh, C.-T.; Li, J.; Ozden, A.; Golam Kibria, M.; Seifitokaldani, A.; Tan, C.-S.; Gabardo, C. M.; Luo, M.; Zhou, H.; Li, F.; Lum, Y.; McCallum, C.; Xu, Y.; Liu, M.; Proppe, A.; Johnston, A.; Todorovic, P.; Zhuang, T.-T.; Sinton, D.; Kelley, S. O.; Sargent, E. H. Catalyst Synthesis under CO2 Electroreduction Favours Faceting and Promotes Renewable Fuels Electrosynthesis. *Nat. Catal.* **2020**, *3*, 98−106.
(44) Schellekens, M. P.; Raaijman, S. J.; T. M. Koper, M. T.; Corbett, P. J. Temperature-Dependent Selectivity for CO Electroreduction on Copper-Based Gas-Diffusion Electrodes at High Current Densities. *Chem. Eng. J.* **2024**, *483*, 149105.
(45) Monis Ayyub, M.; Kormányos, A.; Endrődi, B.; Janáky, C. Electrochemical Carbon Monoxide Reduction at High Current Density: Cell Configuration Matters. *Chem. Eng. J.* **2024**, *490*, 151698.
(46) Romero Cuellar, N. S.; Wiesner-Fleischer, K.; Fleischer, M.; Rucki, A.; Hinrichsen, O. Advantages of CO over CO2 as Reactant for Electrochemical Reduction to Ethylene, Ethanol and n-Propanol on Gas Diffusion Electrodes at High Current Densities. *Electrochim. Acta* **2019**, *307*, 164−175.
(47) Jouny, M.; Luc, W.; Jiao, F. High-Rate Electroreduction of Carbon Monoxide to Multi-Carbon Products. *Nat. Catal.* **2018**, *1*, 748−755.
(48) Li, J.; Wang, Z.; McCallum, C.; Xu, Y.; Li, F.; Wang, Y.; Gabardo, C. M.; Dinh, C.-T.; Zhuang, T.-T.; Wang, L.; Howe, J. Y.; Ren, Y.; Sargent, E. H.; Sinton, D. Constraining CO Coverage on Copper Promotes High-Efficiency Ethylene Electroproduction. *Nat. Catal.* **2019**, *2*, 1124−1131.
(49) Zhu, P.; Xia, C.; Liu, C.-Y.; Jiang, K.; Gao, G.; Zhang, X.; Xia, Y.; Lei, Y.; Alshareef, H. N.; Senftle, T. P.; Wang, H. Direct and Continuous Generation of Pure Acetic Acid Solutions via Electrocatalytic Carbon Monoxide Reduction. *Proc. Natl. Acad. Sci. U.S.A.* **2021**, *118*, No. e2010868118.
(50) Legrand, U.; Apfel, U. P.; Boffito, D. C.; Tavares, J. R. The Effect of Flue Gas Contaminants on the CO2 Electroreduction to Formic Acid. *J. CO2 Util.* **2020**, *42*, 101315.
(51) Wang, H.; Liu, Y.; Laaksonen, A.; Krook-Riekkola, A.; Yang, Z.; Lu, X.; Ji, X. Carbon Recycling - An Immense Resource and Key to a Smart Climate Engineering: A Survey of Technologies, Cost and Impurity Impact. *Renewable Sustainable Energy Rev.* **2020**, *131*, 110010.
(52) Endrődi, B.; Kecsenovity, E.; Samu, A.; Darvas, F.; Jones, R. V.; Török, V.; Danyi, A.; Janáky, C. Multilayer Electrolyzer Stack Converts Carbon Dioxide to Gas Products at High Pressure with High Efficiency. *ACS Energy Lett.* **2019**, *4*, 1770−1777.
(53) Dufek, E. J.; Lister, T. E.; Stone, S. G.; McIlwain, M. E. Operation of a Pressurized System for Continuous Reduction of CO2. *J. Electrochem. Soc.* **2012**, *159*, F514−F517.
(54) Ma, S.; Luo, R.; Gold, J. I.; Yu, A. Z.; Kim, B.; Kenis, P. J. A. Carbon Nanotube Containing Ag Catalyst Layers for Efficient and Selective Reduction of Carbon Dioxide. *J. Mater. Chem. A* **2016**, *4*, 8573−8578.
(55) Wang, R.; Haspel, H.; Pustovarenko, A.; Dikhtiarenko, A.; Russkikh, A.; Shterk, G.; Osadchii, D.; Ould-Chikh, S.; Ma, M.; Smith, W. A.; Takanabe, K.; Kapteijn, F.; Gascon, J. Maximizing Ag Utilization in High-Rate CO 2 Electrochemical Reduction with a Coordination Polymer-Mediated Gas Diffusion Electrode. *ACS Energy Lett.* **2019**, *4*, 2024−2031.
(56) Edwards, J. P.; Xu, Y.; Gabardo, C. M.; Dinh, C.-T.; Li, J.; Qi, Z.; Ozden, A.; Sargent, E. H.; Sinton, D. Efficient Electrocatalytic Conversion of Carbon Dioxide in a Low-Resistance Pressurized Alkaline Electrolyzer. *Appl. Energy* **2020**, *261*, 114305.
(57) Bhargava, S. S.; Proietto, F.; Azmoodeh, D.; Cofell, E. R.; Henckel, D. A.; Verma, S.; Brooks, C. J.; Gewirth, A. A.; Kenis, P. J. A. System Design Rules for Intensifying the Electrochemical Reduction of CO2 to CO on Ag Nanoparticles. *ChemElectroChem* **2020**, *7*, 2001−2011.
(58) Lee, J.; Lee, W.; Ryu, K. H.; Park, J.; Lee, H.; Lee, J. H.; Park, K. T. Catholyte-Free Electroreduction of CO2 for Sustainable Production of CO: Concept, Process Development, Techno-Economic Analysis, and CO2 Reduction Assessment. *Green Chem.* **2021**, *23*, 2397−2410.
(59) Liu, Z.; Yang, H.; Kutz, R.; Masel, R. I. CO2 Electrolysis to CO and O2 at High Selectivity, Stability and Efficiency Using Sustainion Membranes. *J. Electrochem. Soc.* **2018**, *165*, J3371−J3377.
(60) Endrődi, B.; Samu, A.; Kecsenovity, E.; Halmágyi, T.; Sebők, D.; Janáky, C. Operando Cathode Activation with Alkali Metal Cations for High Current Density Operation of Water-Fed Zero-Gap Carbon Dioxide Electrolysers. *Nat. Energy* **2021**, *6*, 439−448.
(61) Monteiro, M. C. O.; Philips, M. F.; Schouten, K. J. P.; Koper, M. T. M. Efficiency and Selectivity of CO2 Reduction to CO on Gold Gas Diffusion Electrodes in Acidic Media. *Nat. Commun.* **2021**, *12*, 4943.
(62) Dinh, C.-T.; García de Arquer, F. P.; Sinton, D.; Sargent, E. H. High Rate, Selective, and Stable Electroreduction of CO2 to CO in Basic and Neutral Media. *ACS Energy Lett.* **2018**, *3*, 2835−2840.
(63) Wang, X.; de Araújo, J. F.; Ju, W.; Bagger, A.; Schmies, H.; Kühl, S.; Rossmeisl, J.; Strasser, P. Mechanistic Reaction Pathways of Enhanced Ethylene Yields during Electroreduction of CO2-CO Co-Feeds on Cu and Cu-Tandem Electrocatalysts. *Nat. Nanotechnol.* **2019**, *14*, 1063−1070.

https://doi.org/10.1021/acs.iecr.5c03012
Ind. Eng. Chem. Res. 2026, 65, 1716−1733

(64) Zhang, B.; Wang, L.; Li, D.; Li, Z.; Bu, R.; Lu, Y. Tandem Strategy for Electrochemical CO2 Reduction Reaction. *Chem Catal.* **2022**, *2*, 3395−3429.
(65) Möller, T.; Filippi, M.; Brückner, S.; Ju, W.; Strasser, P. A CO2 Electrolyzer Tandem Cell System for CO2-CO Co-Feed Valorization in a Ni-N-C/Cu-Catalyzed Reaction Cascade. *Nat. Commun.* **2023**, *14*, 5680.
(66) Romero Cuellar, N. S.; Scherer, C.; Kaçkar, B.; Eisenreich, W.; Huber, C.; Wiesner-Fleischer, K.; Fleischer, M.; Hinrichsen, O. Two-Step Electrochemical Reduction of CO2 towards Multi-Carbon Products at High Current Densities. *J. CO2 Util.* **2020**, *36*, 263−275.
(67) Toth, A. J. N-Propanol Dehydration with Distillation and Pervaporation: Experiments and Modelling. *Membranes (Basel)* **2022**, *12*, 750.
(68) Black, C.; Ditsler, D. E. *Dehydration of Aqueous Ethanol Mixtures by Extractive Distillation*; American Chemical Society: Washington DC, 1974; Vol. *15*, pp 1−15.
(69) Chilev, C.; Lamari, F.; Dicko, M.; Simeonov, E. Investigation of Acetic Acid Dehydration by Various Methods. *J. Chem. Technol. Metall.* **2015**, *51*, 73−84.
(70) James, J.; Lücking, L. E.; van Dijk, H. A. J.; Boon, J. Review of Technologies for Carbon Monoxide Recovery from Nitrogen-Containing Industrial Streams. *Front. Chem. Eng.* **2023**, *5*, 1066091.
(71) Nagahama, K.; Konishi, H.; Hoshino, D.; Hirata, M. Binary Vapour-Liquid Equilibria of Carbon Dioxide-Light Hydrocarbons at Low Temperature. *J. Chem. Eng. Jpn.* **1974**, *7*, 323−328.
(72) Xi, L.; Qianguo, L.; Hasan, M.; Ming, L.; Qiang, L.; Jia, L.; Alisa, W.; Muxin, L.; Francisco, A. Assessing the Economics of CO2 Capture in China's Iron/Steel Sector: A Case Study. *Energy Procedia* **2019**, *158*, 3715−3722.
(73) West, K. *REF BOF Steelmaking—Greenfield—Energy.nl*; Energy.nl, 2024; . https://energy.nl/data/ref-bof-steelmaking-greenfield/ (accessed 2024−02−06.
(74) Zhu, Z.; Xu, B. Purification Technologies for NOx Removal from Flue Gas: A Review. *Separations* **2022**, *9*, 307.
(75) Brandin, J. G. M.; Hulteberg, C. P.; Odenbrand, C. U. I. High-Temperature and High-Concentration SCR of NO with NH3: Application in a CCS Process for Removal of Carbon Dioxide. *Chem. Eng. J.* **2012**, *191*, 218−227.
(76) Sepehrian, M.; Anbia, M.; Hedayatzadeh, M. H.; Yazdi, F. SO2 Dry-Based Catalytic Removal from Flue Gas Leading to Elemental Sulfur Production: A Comprehensive Review. *Process Saf. Environ. Prot.* **2024**, *182*, 456−480.
(77) Poullikkas, A. Review of Design, Operating, and Financial Considerations in Flue Gas Desulfurization Systems. *Energy Technol. Policy* **2015**, *2*, 92−103.
(78) Li, L.; Fan, M.; Brown, R. C.; Koziel, J. A.; van Leeuwen, J. H. Reduction of S02 in Flue Gas and Applications of Fly Ash: A Review. *PowerPlant Chem.* **2008**, *10*, 291−301.
(79) Lim, J.; Kim, J. Designing and Integrating NOx, SO2 and CO2 Capture and Utilization Process Using Desalination Wastewater. *Fuel* **2022**, *327*, 124986.
(80) Wang, Y.; Ding, L.; Long, H.; Xiao, J.; Qian, L.; Wang, H.; Xu, C. C. Carbonyl Sulfur Removal from Blast Furnace Gas: Recent Progress, Application Status and Future Development. *Chemosphere* **2022**, *307*, 136090.
(81) Renda, S.; Barba, D.; Palma, V. Recent Solutions for Efficient Carbonyl Sulfide Hydrolysis: A Review. *Ind. Eng. Chem. Res.* **2022**, *61*, 5685−5697.
(82) Alguacil, F. J. Recent Advances in H2S Removal from Gas Streams. *Appl. Sci.* **2023**, *13*, 3217.
(83) Pudi, A.; Rezaei, M.; Signorini, V.; Andersson, M. P.; Baschetti, M. G.; Mansouri, S. S. Hydrogen Sulfide Capture and Removal Technologies: A Comprehensive Review of Recent Developments and Emerging Trends. *Sep. Purif. Technol.* **2022**, *298*, 121448.
(84) Li, H.; Li, L.; Xu, J.; Li, Y. Selective Absorption of H2S from CO2 Using Sterically Hindered Amines at High Pressure. *Pet. Sci. Technol.* **2019**, *37*, 1825−1829.
(85) Anufrikov, Y. A.; Kuranov, G. L.; Smirnova, N. A. Solubility of CO2 and H2S in Alkanolamine-Containing Aqueous Solutions. *Russ. J. Appl. Chem.* **2007**, *80*, 515−527.
(86) Paulsen, M.; Knuutila, H.; Domenico Pinto, D. D. *Simulation of H2S Removal from Biogas Using Aspen Plus*; NTNU: Trondheim, 2019.
(87) Koytsoumpa, E. I.; Bergins, C.; Kakaras, E. The CO2 Economy: Review of CO2 Capture and Reuse Technologies. *J. Supercrit. Fluids* **2018**, *132*, 3−16.
(88) Liang, Z. H.; Rongwong, W.; Liu, H.; Fu, K.; Gao, H.; Cao, F.; Zhang, R.; Sema, T.; Henni, A.; Sumon, K.; Nath, D.; Gelowitz, D.; Srisang, W.; Saiwan, C.; Benamor, A.; Al-Marri, M.; Shi, H.; Supap, T.; Chan, C.; Zhou, Q.; Abu-Zahra, M.; Wilson, M.; Olson, W.; Idem, R.; Tontiwachwuthikul, P. Recent progress and new developments in post-combustion carbon-capture technology with amine based solvents. *Int. J. Greenhouse Gas Control* **2015**, *40*, 26−54.
(89) Ramdin, M.; Morrison, A. R. T.; de Groen, M.; van Haperen, R.; de Kler, R.; Irtem, E.; Laitinen, A. T.; van den Broeke, L. J. P.; Breugelmans, T.; Trusler, J. P. M.; De Jong, W.; Vlugt, T. J. H. High-Pressure Electrochemical Reduction of CO2 to Formic Acid/Formate: Effect of PH on the Downstream Separation Process and Economics. *Ind. Eng. Chem. Res.* **2019**, *58*, 22718−22740.
(90) Li, B.-H.; Zhang, N.; Smith, R. Simulation and Analysis of CO2 Capture Process with Aqueous Monoethanolamine Solution. *Appl. Energy* **2016**, *161*, 707−717.
(91) Garcia, M.; Knuutila, H. K.; Gu, S. ASPEN PLUS Simulation Model for CO2 Removal with MEA: Validation of Desorption Model with Experimental Data. *J. Environ. Chem. Eng.* **2017**, *5*, 4693−4701.
(92) Küngas, R. Review-Electrochemical CO 2 Reduction for CO Production: Comparison of Low- and High-Temperature Electrolysis Technologies. *J. Electrochem. Soc.* **2020**, *167*, 044508.
(93) Gao, F.-Y.; Bao, R.-C.; Gao, M.-R.; Yu, S.-H. Electrochemical CO 2 -to-CO Conversion: Electrocatalysts, Electrolytes, and Electrolyzers. *J. Mater. Chem. A* **2020**, *8*, 15458−15478.
(94) Ren, C.; Ni, W.; Li, H. Recent Progress in Electrocatalytic Reduction of CO2. *Catalysts* **2023**, *13*, 644.
(95) O'Brien, C. P.; Miao, R. K.; Liu, S.; Xu, Y.; Lee, G.; Robb, A.; Huang, J. E.; Xie, K.; Bertens, K.; Gabardo, C. M.; Edwards, J. P.; Dinh, C.-T.; Sargent, E. H.; Sinton, D. Single Pass CO2 Conversion Exceeding 85% in the Electrosynthesis of Multicarbon Products via Local CO2 Regeneration. *ACS Energy Lett.* **2021**, *6*, 2952−2959.
(96) Greenblatt, J. B.; Miller, D. J.; Ager, J. W.; Houle, F. A.; Sharp, I. D. The Technical and Energetic Challenges of Separating (Photo)-Electrochemical Carbon Dioxide Reduction Products. *Joule* **2018**, *2*, 381−420.
(97) Zhu, L.-Y.; Li, Y.-C.; Liu, J.; He, J.; Wang, L.-Y.; Lei, J.-D. Recent Developments in High-Performance Nafion Membranes for Hydrogen Fuel Cells Applications. *Pet. Sci.* **2022**, *19*, 1371−1381.
(98) Zakil, F. A.; Kamarudin, S. K.; Basri, S. Modified Nafion Membranes for Direct Alcohol Fuel Cells: An Overview. *Renewable Sustainable Energy Rev.* **2016**, *65*, 841−852.
(99) Dutta, N. N.; Patil, G. S. Developments in CO Separation. *Gas Sep. Purif.* **1995**, *9*, 277−283.
(100) Ma, X.; Albertsma, J.; Gabriels, D.; Horst, R.; Polat, S.; Snoeks, C.; Kapteijn, F.; Eral, H. B.; Vermaas, D. A.; Mei, B.; de Beer, S.; van der Veen, M. A. Carbon Monoxide Separation: Past, Present and Future. *Chem. Soc. Rev.* **2023**, *52*, 3741−3777.
(101) Yousefi, M.; Azizi, S.; Peyghambarzadeh, S. M.; Azizi, Z. Intensification of Ethylene and Ethane Absorption in N-Methyl-2-Pyrrolidone (NMP) by Adding Silver Nanoparticles. *Chem. Eng. Process.* **2020**, *158*, 108184.
(102) Bachman, J. E.; Reed, D. A.; Kapelewski, M. T.; Chachra, G.; Jonnavittula, D.; Radaelli, G.; Long, J. R. Enabling Alternative Ethylene Production through Its Selective Adsorption in the Metal-Organic Framework Mn2(m-Dobdc). *Energy Environ. Sci.* **2018**, *11*, 2423−2431.
(103) Xie, Y. C.; Zhang, J.; Geng, Y.; Tang, W.; Tong, X. Z. Large Scale CO Separation by VPSA Using CuCl/Zeolite Adsorbent. In *Adsorption*; World Scientific, 2007; pp 245−252.

https://doi.org/10.1021/acs.iecr.5c03012
Ind. Eng. Chem. Res. 2026, 65, 1716−1733

(104) Chen, Y.; Ning, P.; Xie, Y.; Chen, Y.; Sun, H.; Lie, Z. Pilot-Scale Experiment for Purification of CO from Industrial Tail Gases by Pressure Swing Adsorption. *Chin. J. Chem. Eng.* **2008**, *16*, 715−721.
(105) Xiao, P.; Zhang, J.; Webley, P.; Li, G.; Singh, R.; Todd, R. Capture of CO2 from Flue Gas Streams with Zeolite 13X by Vacuum-Pressure Swing Adsorption. *Adsorption* **2008**, *14*, 575−582.
(106) Faraji, S.; Gharebagh, R. S.; Mostoufi, N. Hydrogen Recovery from Refinery Off-Gases. *J. Appl. Sci.* **2005**, *5*, 459−464.
(107) Moral, G.; Ortiz, A.; Gorri, D.; Ortiz, I. Hydrogen Recovery from Industrial Waste Streams Using Matrimid/ZIF Mixed Matrix Membranes. *Int. J. Hydrogen Energy* **2024**, *51*, 210−224.
(108) David, O. C.; Gorri, D.; Urtiaga, A.; Ortiz, I. Mixed Gas Separation Study for the Hydrogen Recovery from H2/CO/N2/CO2 Post Combustion Mixtures Using a Matrimid Membrane. *J. Membr. Sci.* **2011**, *378*, 359−368.
(109) Pettersen, T.; Lien, K. M. A New Robust Design Model for Gas Separating Membrane Modules, Based on Analogy with Counter-Current Heat Exchangers. *Comput. Chem. Eng.* **1994**, *18*, 427−439.
(110) Al-Rabiah, A. A.; Timmerhaus, K. D.; Noble, R. D. Membrane Technology for Hydrogen Separation in Ethylene Plants. In *6th World Congress of Chemical Engineering*: Melbourne, 2001; pp 1−7.
(111) Peer, M.; Mehdi Kamali, S.; Mahdeyarfar, M.; Mohammadi, T. Separation of Hydrogen from Carbon Monoxide Using a Hollow Fiber Polyimide Membrane: Experimental and Simulation. *Chem. Eng. Technol.* **2007**, *30*, 1418−1425.
(112) Mazzotti, M.; Gazzani, M.; Milella, F.; Gabrielli, P. *Membrane Separations Rate Controlled Separation Processes*; ETH Zurich, 2016.
(113) Hartanto, D.; Sutrisno, A.; Widya, V.; Mustain, A.; Handayani, P. A.; Prasetiawan, H.; Chafidz, A.; Khoiroh, I. Simulation of the Extractive Distillation Using Ethylene Glycol as an Entrainer in the Bioethanol Dehydration. In *Proceedings of the 7th Engineering International Conference on Education, Concept and Application on Green Technology*; SCITEPRESS—Science and Technology Publications, 2018; pp 450−454.
(114) Villarroel Rojas, J.; Stinguel, L.; Wolf-Maciel, M. R.; Guirardello, R. Modeling and Simulating Complete Extractive Distillation Process of Ethanol-Water Mixture Using Equilibrium-Stage Distillation Model and Efficiency Correlations (Barros & Wolf) on EMSO Platform. *Chem. Eng. Trans.* **2016**, *50*, 331−336.
(115) Wu, Y.; Meng, D.; Yao, D.; Liu, X.; Xu, Y.; Zhu, Z.; Wang, Y.; Gao, J. Mechanism Analysis, Economic Optimization, and Environmental Assessment of Hybrid Extractive Distillation-Pervaporation Processes for Dehydration of n -Propanol. *ACS Sustain. Chem. Eng.* **2020**, *8*, 4561−4571.
(116) Pla-Franco, J.; Lladosa, E.; Loras, S.; Montón, J. B. Approach to the 1-Propanol Dehydration Using an Extractive Distillation Process with Ethylene Glycol. *Chem. Eng. Process.* **2015**, *91*, 121−129.
(117) Pla-Franco, J.; Lladosa, E.; Loras, S.; Montón, J. B. Azeotropic Distillation for 1-Propanol Dehydration with Diisopropyl Ether as Entrainer: Equilibrium Data and Process Simulation. *Sep. Purif. Technol.* **2019**, *212*, 692−698.
(118) Liu, S.; Li, H.; Kruber, B.; Skiborowski, M.; Gao, X. Process Intensification by Integration of Distillation and Vapor Permeation or Pervaporation - An Academic and Industrial Perspective. *Results Eng.* **2022**, *15*, 100527.
(119) Zhang, H.; Jiao, Y.; Zhao, Q.; Li, C.; Cui, P.; Wang, Y.; Zheng, S.; Li, X.; Zhu, Z.; Gao, J. Sustainable Separation of Ternary Azeotropic Mixtures Based on Enhanced Extractive Distillation/Pervaporation Structure and Multi-Objective Optimization. *Sep. Purif. Technol.* **2022**, *298*, 121685.
(120) Xue, S.; Wu, C.; Wu, Y.; Chen, J.; Li, Z. Bipolar Membrane Electrodialysis for Treatment of Sodium Acetate Waste Residue. *Sep. Purif. Technol.* **2015**, *154*, 193−203.
(121) Chukwu, U. N.; Cheryan, M. Electrodialysis of Acetate Fermentation Broths. *Appl. Biochem. Biotechnol.* **1999**, *78*, 485−500.
(122) Suwal, S.; Li, J.; Engelberth, A. S.; Huang, J.-Y. Application of Electro-Membrane Separation for Recovery of Acetic Acid in Lignocellulosic Bioethanol Production. *Food Bioprod. Process.* **2018**, *109*, 41−51.
(123) Karunanithi, S.; Kapoor, A.; Senthil Kumar, P.; Balasubramanian, S.; Rangasamy, G. Solvent Extraction of Acetic Acid from Aqueous Solutions: A Review. *Sep. Sci. Technol.* **2023**, *58*, 1985−2007.
(124) Park, S.-J.; Moon, J.-K.; Um, B.-H. Evaluation of the Efficiency of Solvent Systems to Remove Acetic Acid Derived from Pre-Pulping Extraction. *J. Korean Wood Sci. Technol.* **2013**, *41*, 447−455.
(125) Li, K.-L.; Chien, I.-L.; Cheng-Liang, C. Design and Optimization of Acetic Acid Dehydration Processes. In *Advanced Control of Industrial Processes*; ADCON: Hiroshima, Japan, 2014; pp 126−131.
(126) Sievert, K.; Schmidt, T. S.; Steffen, B. Considering Technology Characteristics to Project Future Costs of Direct Air Capture. *Joule* **2024**, *8*, 979−999.
(127) Young, J.; McQueen, N.; Charalambous, C.; Foteinis, S.; Hawrot, O.; Ojeda, M.; Pilorgé, H.; Andresen, J.; Psarras, P.; Renforth, P.; Garcia, S.; van der Spek, M. The Cost of Direct Air Capture and Storage Can Be Reduced via Strategic Deployment but Is Unlikely to Fall below Stated Cost Targets. *One Earth* **2023**, *6*, 899−917.
(128) Trading Economics *EU Natural Gas TTF-Price-Chart-Historical Data-News* 2025. https://tradingeconomics.com/commodity/eu-natural-gas (accessed 2025−10−18).
(129) Bains, P.; Psarras, P.; Wilcox, J. CO2 Capture from the Industry Sector. *Prog. Energy Combust. Sci.* **2017**, *63*, 146−172.
(130) Aromada, S. A.; Eldrup, N. H.; Erik Øi, L. Capital Cost Estimation of CO2 Capture Plant Using Enhanced Detailed Factor (EDF) Method: Installation Factors and Plant Construction Characteristic Factors. *Int. J. Greenhouse Gas Control* **2021**, *110*, 103394.
(131) *European Power Price Tracker*; Ember, 2024. https://ember-climate.org/data/data-tools/europe-power-prices/ (accessed 2024−07−08).
(132) *Electricity Price Netherlands 2024*; Statista Research Department, 2024. https://www.statista.com/statistics/1314549/netherlands-monthly-wholesale-electricity-price/ (accessed 2024−07−08).
(133) Xing, X.; Cong, Y.; Wang, Y.; Wang, X.; Cong, Y.; Wang, Y.; Wang, X. The Impact of COVID-19 and War in Ukraine on Energy Prices of Oil and Natural Gas. *Sustainability* **2023**, *15*, 14208.
(134) Foerter, D.; Jozewicz, W. *Cost of Selective Catalytic Reduction (SCR) Application for NOx Control on Coal-Fired Boilers*; U.S. Environmental Protection Agency, Office of Research and Development: Washington, DC, 2001.
(135) Dingler, J. E.; Nirula, S.; Sedriks, W. *Costs of Synthesis Gases and Methanol - Chemical Production and Investment Cost*; S&P Global: Menlo Park, CA, 1983.
(136) Luyben, W. L. Capital Cost of Compressors for Conceptual Design. *Chem. Eng. Process.* **2018**, *126*, 206−209.
(137) Woods, D. R. *Rules of Thumb in Engineering Practice*; Wiley, 2007.
(138) Alqaheem, Y.; Alomair, A. Hydrogen Recovery from ARDS Unit by Membranes: A Simulation and Economic Study. *Results Eng.* **2022**, *15*, 100559.
(139) Lin, H.; He, Z.; Sun, Z.; Kniep, J.; Ng, A.; Baker, R. W.; Merkel, T. C. CO2-Selective Membranes for Hydrogen Production and CO2 Capture - Part II: Techno-Economic Analysis. *J. Membr. Sci.* **2015**, *493*, 794−806.
(140) Ankoliya, D.; Mudgal, A.; Sinha, M. K.; Davies, P.; Park, K.; Alegre, R. R.; Patel, V.; Patel, J. Techno-Economic Analysis of Integrated Bipolar Membrane Electrodialysis and Batch Reverse Osmosis for Water and Chemical Recovery from Dairy Wastewater. *J. Cleaner Prod.* **2023**, *420*, 138264.
(141) Lee, J. Y.; Chen, P. Y. Optimization of Heat Recovery Networks for Energy Savings in Industrial Processes. *Processes* **2023**, *11*, 321.
(142) Jegla, Z.; Freisleben, V. Practical Energy Retrofit of Heat Exchanger Network Not Containing Utility Path. *Energies (Basel)* **2020**, *13*, 2711.
(143) IRENA *International Co-Operation to Accelerate Green Hydrogen Deployment*; IRENA: Abu Dhabi, 2024. https://www.irena.org/

https://doi.org/10.1021/acs.iecr.5c03012
Ind. Eng. Chem. Res. 2026, 65, 1716−1733

Publications/2024/Apr/International-co-operation-to-accelerate-green-hydrogen-deployment (accessed 2024−07−12).
(144) IEA *Global Hydrogen Review 2023*; IEA: Paris, 2023. https://www.iea.org/reports/global-hydrogen-review-2023 (accessed 2024−07−12).
(145) Schmitt, A.; Zhou, H. *EU Energy Outlook to 2060: How will Power Prices and Revenues Develop for Wind, Solar, Gas, Hydrogen + More—Energy Post*; Montel, 2024. https://energypost.eu/eu-energy-outlook-to-2060-how-will-power-prices-and-revenues-develop-for-wind-solar-gas-hydrogen-more/ (accessed 2024−07−12).
(146) Biber, A.; Felder, M.; Wieland, C.; Spliethoff, H. Negative Price Spiral Caused by Renewables? Electricity Price Prediction on the German Market for 2030. *Electr. J.* **2022**, *35*, 107188.
(147) *Ethylene Price Index*; businessanalytiq, 2024. https://businessanalytiq.com/procurementanalytics/index/ethylene-price-index/ (accessed 2024−07−12).
(148) *Ethanol Price Index*; businessanalytiq, 2024. https://businessanalytiq.com/procurementanalytics/index/ethanol-price-index/ (accessed 2024−07−12).
(149) *n-Propanol (1-Propanol) Price Index*; businessanalytiq, 2024. https://businessanalytiq.com/procurementanalytics/index/npropanol-price-index/ (accessed 2024−07−12).
(150) *Acetic Acid Price Index*; businessanalytiq, 2024. https://businessanalytiq.com/procurementanalytics/index/acetic-acid-price-index/ (accessed 2024−07−12).
(151) *Green Hydrogen Price Index*; businessanalytiq, 2024. https://businessanalytiq.com/procurementanalytics/index/green-hydrogen-price-index/ (accessed 2024−07−12).
(152) Slome, S. *Making Money out of Thin Air: Valorizing the Oxygen Byproduct of Green Hydrogen Production*; NexantECA. https://www.nexanteca.com/blog/202401/making-money-out-thin-air-valorizing-oxygen-byproduct-green-hydrogen-production (accessed 2024−07−12.
(153) Münster, M.; Bramstoft, R.; Kountouris, I.; Langer, L.; Keles, D.; Schlautmann, R.; Mörs, F.; Saccani, C.; Guzzini, A.; Pellegrini, M.; Zauner, A.; Böhm, H.; Markova, D.; You, S.; Pumpa, M.; Fischer, F.; Sergi, F.; Brunaccini, G.; Aloisio, D.; Ferraro, M.; Mulder, M.; Rasmusson, H. Perspectives on Green Hydrogen in Europe-during an Energy Crisis and towards Future Climate Neutrality. *Oxford Open Energy* **2024**, *3*, oiae001.
(154) WEC. *Working Paper: Hydrogen Demand and Cost Dynamics*; World Energy Council; London, 2021. https://www.worldenergy.org/publications/entry/working-paper-hydrogen-demand-and-cost-dynamics (accessed 2024−07−17).
(155) Overa, S.; Feric, T. G.; Park, A.-H. A.; Jiao, F. Tandem and Hybrid Processes for Carbon Dioxide Utilization. *Joule* **2021**, *5*, 8−13.
(156) Ozden, A.; Wang, Y.; Li, F.; Luo, M.; Sisler, J.; Thevenon, A.; Rosas-Hernández, A.; Burdyny, T.; Lum, Y.; Yadegari, H.; Agapie, T.; Peters, J. C.; Sargent, E. H.; Sinton, D. Cascade CO2 Electroreduction Enables Efficient Carbonate-Free Production of Ethylene. *Joule* **2021**, *5*, 706−719.
(157) Kibria Nabil, S.; McCoy, S.; Kibria, M. G. Comparative Life Cycle Assessment of Electrochemical Upgrading of CO2 to Fuels and Feedstocks. *Green Chem.* **2021**, *23*, 867−880.
(158) Verma, S.; Lu, S.; Kenis, P. J. A. Co-Electrolysis of CO2 and Glycerol as a Pathway to Carbon Chemicals with Improved Technoeconomics Due to Low Electricity Consumption. *Nat. Energy* **2019**, *4*, 466−474.
(159) Khan, M. A.; Nabil, S. K.; Al-Attas, T. A.; Hu, J.; Kibria, M. G. Electrochemical Reduction of CO 2 to Ethylene with Coproduction of Glycolic Acid Via Glycerol Oxidation. *ECS Meet. Abstr.* **2021**, *MA2021-01*, 1277.
(160) Wang, G.; Chen, J.; Li, K.; Huang, J.; Huang, Y.; Liu, Y.; Hu, X.; Zhao, B.; Yi, L.; Jones, T. W.; Wen, Z. Cost-Effective and Durable Electrocatalysts for Co-Electrolysis of CO2 Conversion and Glycerol Upgrading. *Nano Energy* **2022**, *92*, 106751.
(161) van Bavel, S.; Verma, S.; Negro, E.; Bracht, M. Integrating CO 2 Electrolysis into the Gas-to-Liquids-Power-to-Liquids Process. *ACS Energy Lett.* **2020**, *5*, 2597−2601.

https://doi.org/10.1021/acs.iecr.5c03012
Ind. Eng. Chem. Res. 2026, 65, 1716−1733